

2. BASIS FOR THE FIELD STUDY PLAN

This section describes the central California study area, the magnitudes and locations of ozone concentrations and their chemical components, emissions sources, meteorology that affects ozone levels, and applicable transformation chemistry of the study area. It integrates this knowledge into a “conceptual model” of the phenomena that should be reproduced by the regulatory ozone models.

2.1 CCOS Study Area

Central California is a complex region for air pollution, owing to its proximity to the Pacific Ocean, its diversity of climates, and its complex terrain. Figure 2.1-1 shows the overall study domain with major landmarks, mountains and passes. Figure 2.1-2 shows major political boundaries, including cities, counties, air quality planning districts, roads, Class 1 (pristine) areas, and military facilities. The Bay Area, southern Sacramento Valley, San Joaquin Valley, central portion of the Mountain Counties Air Basin (MCAB), and the Mojave Desert are currently classified as nonattainment for the federal 1-hour ozone NAS. With the exception of Plumas and Sierra Counties in the MCAB, Lake County, and the North Coast, the entire study domain is currently nonattainment for the state 1-hour ozone standard. The Mojave Desert inherits poor air quality generated in the other parts of central and southern California.

The Bay Area Air Quality Management District (BAAQMD) encompasses an area of more than 14,000 km² of which 1,450 km² are the San Francisco and San Pablo Bays, 300 km² are the Sacramento and San Joaquin river deltas, 9,750 km² are mountainous or rural, and 2,500 km² are urbanized. The Bay Area is bounded on the west by the Pacific Ocean, on the east by the Mt. Hamilton and Mt. Diablo ranges, on the south by the Santa Cruz Mountains, and on the north by the northern reaches of the Sonoma and Napa Valleys. The San Joaquin Valley lies to the east of the BAAQMD, and major airflows between the two air basins occur at the Sacramento delta, the Carquinez Strait, and Altamont Pass (elevation 304 m). The coastal mountains have nominal elevations of 500 m, although major peaks are much higher (Mt. Diablo, 1,173 m; Mt. Tamalpais, 783 m; Mt. Hamilton, 1,328 m). Bays and inland valleys punctuate the coastal mountains, including San Pablo Bay, San Francisco Bay, San Ramon Valley, Napa Valley, Sonoma Valley, and Livermore Valley. Many of these valleys and the shorelines of the bays are densely populated. The Santa Clara, Bear, and Salinas Valleys lie to the south of the BAAQMD, containing lower population densities and larger amounts of agriculture.

The BAAQMD manages air quality in Alameda, Contra Costa, Marin, San Francisco, San Mateo, Santa Clara, and Napa counties, in the southern part of Sonoma county, and in the southwestern portion of Solano county. More than six million people, approximately 20% of California’s population, reside within this jurisdiction. The Bay Area contains some of California’s most densely populated incorporated cities, including San Francisco (pop. ~724,000), San Jose (pop. ~782,000), Fremont (pop. ~173,000), Oakland (pop. ~372,000), and Berkeley (pop. ~103,000). In total, over 100 incorporated cities lie within the jurisdiction of the BAAQMD.

Major industries and areas of employment in the Bay Area include tourism, government/defense, electronics manufacturing, software development, agriculture (vineyards, orchards, livestock), petroleum-refining, power generation, and steel manufacturing. BAAQMD residences are often distant from employment locations. More than 1,800 km of major controlled-access highways and bridges accommodate approximately 148 million vehicle miles traveled on a typical weekday. The Bay Area includes a diverse mixture of income levels, ethnic heritages, and lifestyles.

Sacramento Valley

Mountain Counties

The San Joaquin Valley, administered by the San Joaquin Valley Unified Air Pollution Control District (SJVUAPCD), is much larger than the Bay Area but with a lower population. It encompasses nearly 64,000 km² and contains a population in excess of three million people, with a much lower density than that of the Bay Area. The majority of this population is centered in the large urban areas of Bakersfield (pop. ~175,000), Fresno (pop. ~355,000), Modesto (pop. ~165,000), and Stockton (pop. ~211,000). There are nearly 100 smaller communities in the region and many isolated residences surrounded by farmland.

The SJV is bordered on the west by the coastal mountain range, rising to 1,530 meters (m) above sea level (ASL), and on the east by the Sierra Nevada range with peaks exceeding 4,300 m ASL. These ranges converge at the Tehachapi Mountains in the southernmost end of the valley with mountain passes to the Los Angeles basin (Tejon Pass, 1,256 m ASL) and to the Mojave Desert (Tehachapi Pass, 1,225 m ASL, Walker Pass, 1609 m ASL). Agriculture of all types is the major industry in the SJV. Oil and gas production, refining, waste incineration, electrical co-generation, transportation, commerce, local government and light manufacturing constitute the remainder of SJV the economy. Cotton, alfalfa, corn, safflower, grapes, and tomatoes are the major crops. Cattle feedlots, dairies, chickens, and turkeys constitute most of the animal husbandry in the region.

The Mojave Desert is located in southeastern California, north of the Los Angeles metropolitan area and west of California's San Joaquin Valley. It is bordered on the west by the Sierra Nevadas and Tehachapi Mountains and on the south by the San Gabriel and San Bernardino Mountains. The long and narrow valleys of Owens, Panamint, and Death Valley lie to the north. The Mojave Desert is punctuated by a series of mountains and playas to the east, and reaches as far as Las Vegas, NV. The typical elevation of the desert is 500 to 1,000 m ASL.

The Mojave Desert occupies more than 60,000 km² and contains nearly all of San Bernardino county (excluding the city of San Bernardino), the portion of Kern county west of the Tehachapi Mountains, and the portion of Los Angeles county north of the San Gabriel Mountains. It is sparsely populated compared to the neighboring air basins, with approximately 500,000 people. Most of these people live in suburbs of Los Angeles, including Apple Valley (pop. 48,000), Hesperia (pop. 50,000), Lancaster (pop. 97,000), Palmdale (pop. 69,000), and

Victorville (pop. 40,000). Other cities of significance in the Mojave Desert have smaller populations, including Barstow (pop. 21,000), California City (pop. 6,000), Mojave (pop. 3,800), Ridgecrest (pop. 28,000), Rosamond (pop. 7,400), and Tehachapi (pop. 5,800). Several smaller communities are interspersed among these population centers.

The Mojave Desert's aridity, large flat valleys (many of which contain dry lakebeds), low population densities, and isolation made it a good location for military facilities. The U.S. Department of Defense (DOD) operates Edwards and George Air Force Bases, the China Lake Naval Weapons Center, and the Fort Irwin Army National Training Center in the Mojave Desert. Nearly the entire area of the Mojave Desert and a lower portion of the Sierra Nevadas are designated as the R2508 airspace. Excluding Los Angeles commuters, the majority of employment is associated with military and aerospace activities. Recreation and leisure have been growing industries in recent years. A major mineral mining and processing facility is located in Trona, about 70 km east of Ridgecrest and several large cement facilities are located in the Barstow vicinity.

Figure 2.1-3 shows the major population centers in central California, while Table 2.1-1 summarizes populations for Metropolitan Statistical Areas (MSA). Figure 2.1-4 shows land use within central California. There are substantial tracts of grazed and ungrazed forest and woodland along the Pacific coast and in the Sierra Nevadas. Cropland with grazing and irrigated cropland dominate land use in the San Joaquin Valley, while desert scrubland is the dominant land use east of Tehachapi Pass. Tanner et al. (1992) show the various vegetation classes determined from satellite imagery. The central portion of the SJV is intensively farmed; the periphery consists of open pasture into the foothills of the coastal ranges and the Sierra Nevadas. As elevations increase above 400 m, the vegetation progresses through chaparral to deciduous and coniferous trees.

Central California contains the state's major transportation routes, as shown in Figure 2.1-5. The western and central lengths of the SJV are traversed by Interstate 5 and State Route 99. U.S. Highway 101 is aligned with the south central coast, then through the Salinas Valley, through the Bay Area and further north. These are the major arteries for both local and long-distance passenger and commercial traffic. Major east-west routes include I 80 and SR 120, 152, 198, 46, and 58. Many smaller arteries, both paved and unpaved, cross the SJV on its east side, although there are few of these small roads on the western side. The major cities contain a mixture of expressways, surface connectors, and residential streets. Farmland throughout the region contains private lanes for the passage of off-road implements and large trucks that transport agricultural products to market.

2.2 Ambient Trends in Ozone and Precursor Gases

An analysis of ozone trends over the CCOS study region was undertaken to examine the changes in mean and maximum daily ozone concentration and the frequency of occurrence of exceedances of the Federal 1-hr and proposed 8-hr ozone standards over the years 1990-1998. An abbreviated analysis of ozone precursors, i.e., non-methane hydrocarbons (NMHC) and oxides of nitrogen (NO_x), is also presented.

2.2.1 Trends in Ozone Exceedances

A database was obtained from all stations reporting ozone measurements listed in the California Air Resources Board Aerometric Data Analysis and Management (ADAM) System for 1990-1998. (Data supplied courtesy of Dwight Oda, ARB). For each available day during the nine ozone seasons, defined as May-October for this investigation, the 1-hour and 8-hour maximum ozone concentrations and the start-time of the 1-hr and 8-hour peak ozone were compiled. From the 207 sites in the ADAM database, a subset of 153 sites was selected based on period of record, the acceptability of linking nearby sites to gain a longer period of record, the data recovery rate during the 1996-1998 ozone seasons, and the expected continuation of monitoring at that site into the summer 2000 CCOS field study period. Twenty-seven sites, satisfying the criteria of close proximity and similar ozone temporal patterns were linked in time to an in-service site, providing 126 “linked ADAM” sites (assigned a “LADAM#” equivalent to the ARB ADAM# number of the most recent site). This linked master list is shown in Table 2.2-1a. Included in Table 2.2-1a is information on the three functional site location types, Urban/City Center, Suburban, or Rural. Documentation and details of linking these sites is provided in Table 2.2-1b.

Table 2.2-2 gives a summary of 1-hour and 8-hour mean maximum daily ozone for the years 1990-1998 by air basin. All reporting sites for the air basin in each year were used to compile the mean of daily 1-hour and 8-hour maxima and the basin-wide average of daily maxima. Three annual groupings are also provided for 1990-1995, 1996-1998, and the entire nine-year period, but only years with >75% data recovery are included in the group means. Table 2.2-3 shows the annual maximum and mean average daily maximum for each site. Figures 2.2-1 and 2.2-2 summarize mean ozone trends by location type and by weekday across all basins. Figure 2.2-2 is not a rigorous statistical treatment, since the distribution of daily ozone maxima across basins are skewed somewhat from normal, but the large number of cases (over 9000 for Rural and Suburban locations, and over 6000 for Urban/City) in each average provide compelling evidence of the effect.

Tables 2.2-4 through 2.2-7 give a breakdown, by site in each air basin, of 1hr and 8hr exceedance annual trends, seasonal occurrences by month (May-Oct), diurnal distribution of exceedances by start hour (PST), and the hebdomadal cycle, respectively. Several features are evident from the tables:

- Sites downwind of Sacramento have the greatest number of exceedances per year in the SV and MC air basins, i.e., Folsom and Auburn in SV, and Cool and Placerville in MC.
- Sites downwind of Bakersfield (Arvin and Edison) and Fresno (Parlier and Maricopa) have the greatest number of exceedances per year in the SJV air basin, with more exceedances per season in the south SJV basin. Southern SJV has the worst air quality in the CCOS region.
- Healdsburg, Livermore, Pinnacles National Monument, and Simi Valley, have the highest exceedances per season of both the 1-hr and 8-hr standards for NC, SFBA, NCC, and SCC air basins, respectively.

- Air quality is in attainment in the LC and NEP basins, and northern portions of the NC meet the standards.
- The El Nino event during 1997 significantly lowered the number of exceedances of both the 1hr and 8hr standards in the NCC, SV, and SFBA basins. In fact, no 1hr or 8hr exceedances occurred in SFBA during 1997. However, this El Nino effect is not evident for all sites in the SJV and SCC basins, particularly for sites closer to the South Coast air basin.
- By inspection, July and August are approximately equal in the number of exceedances per month, for both the 1hr and 8hr standards, at most sites in the study domain. Similarly, June and September are approximately equal. Notable exceptions include more September than June exceedances in the southern SJV, and more June than September exceedances at all MD sites.
- Daily 1hr ozone maxima by start time shows the usual pattern of peak ozone near solar noon in the source regions, with increasing later times for downwind receptor sites. This is also true for the 8hr maxima in Table 2.2-6b, except that the start times are shifted forward by 3-4 hours relative to the respective 1hr maxima.
- Subtle weekday/weekend differences are not immediately obvious by inspection of Table 2.2-7. Figure 2.2-2 provides more detail, but a rigorous statistical analysis is beyond the scope of this conceptual plan.

2.2.2 Spatial and Temporal Patterns of Ozone Precursors

Graphs have been prepared on NMHC and NO_x trends and will be presented at the June 11, 1999 Technical Committee meeting in Sacramento. A discussion of these will also be incorporated in the next draft. One major finding is the marked reduction in NMHC at some sites during the 1997 season.

2.3 Emissions and Source Contributions

Section 39607(b) of the California Health and Safety Code requires the California Air Resources Board (ARB) to inventory sources of air pollution within the 14 air basins of the state and to determine the kinds and quantities of pollutants that come from those sources. The pollutants inventoried are total organic gases (TOG), reactive organic gases (ROG), carbon monoxide (CO), oxides of nitrogen (NO_x), oxides of sulfur (SO_x), and particulate matter with an aerodynamic diameter of 10 micrometers or smaller (PM₁₀). TOG consist of hydrocarbons including methane, aldehydes, ketones, organic acids, alcohol, esters, ethers, and other compounds containing hydrogen and carbon in combination with one or more other elements. ROG include all organic gases except methane and a number of organic compounds such as low molecular weight halogenated compounds that have been identified by the U.S. Environmental Protection Agency (EPA) as essentially non-reactive. For ROG and PM₁₀, the emission estimates are calculated from TOG and PM, respectively, using reactive organic fractions and

particle size fractions. Emission sources are categorized as on-road mobile sources, non-road mobile sources, stationary point sources, stationary area sources, and natural sources.

The emission inventory for 1996 is the most recent compilation published by the California Air Resources Board. Point source emission estimates in the inventory were provided by the air pollution control districts and the air quality management districts. Area source emission estimates were made by either the districts or the ARB staffs. On-road motor vehicle emission estimates were made by the ARB staff. The emission estimates are in tons per average day, determined by dividing annual emissions by 365. The estimates have been rounded off to two significant figures.

Tables 2.3-1 and 2.3-2 show the daily averages by air basin for ROG and NO_x emissions, respectively (California Air Resources Board, 1998). Emissions in the CCOS area in 1996 total 1575 and 1545 tons/day for ROG and NO_x, respectively, with 80 and 84 percent of those pollutants emitted within the three major air basins, Bay Area, Sacramento Valley and San Joaquin Valley. Stationary and area sources, together, contribute equally to ROG emissions as do mobile sources, while mobile sources account for the majority of NO_x emissions (74 percent from mobile).

2.4 Summer Ozone Climatology

Given the primary emissions within central California, it is the local climate of California that fosters generation of ozone, a secondary pollutant. High ozone concentrations most frequently occur during the “ozone season,” spanning late spring, summer, and early fall when sunlight is most abundant. Meteorology is the dominant factor controlling the change in ozone air quality from one day to the next. Synoptic and mesoscale meteorological features govern the transport of emissions between sources and receptors, affecting the dilution and dispersion of pollutants during transport and the time available during which pollutants can react with one another to form ozone. These features are important to transport studies and modeling efforts owing to their influence on reactive components and ozone formation and deposition. This subsection provides a summary of meteorological features affecting central California air quality, and provides a brief overview of the regulatory response to inter-basin transport, i.e., the identification of “transport couples” and the characterization of the effect of transport on air quality in the receptor air basin. Specific transport studies are discussed in greater detail with the introduction of transport scenarios of interest.

2.4.1 Typical Large-Scale Meteorological Features

General descriptions of meteorological effects on California air quality abound in the literature (e.g., Ahrens, 1988). For the San Joaquin Valley, the 1990 SJVAQS/AUSPEX/SARMAP bibliography prepared by Solomon et al (1997) is comprehensive. Briefly, the summer climatology of central California is generally dominated by the semi-permanent Eastern Pacific High-Pressure System. This synoptic feature is manifest as a dome of warm air (a maximum in the 500-mb geopotential height field) with a surrounding anticyclonic circulation (clockwise in the Northern Hemisphere). Therefore, surface winds blow clockwise and outward from the high, a motion associated with low-level divergence, and therefore sinking motion aloft and fair weather. This sinking motion also gives rise to adiabatic heating and

therefore warm temperatures aloft. A key indicator of this warm, capping subsidence inversion in California is the temperature of the 850-mb pressure surface from the Oakland soundings. This single meteorological variable from the 0400 PST sounding is perhaps best correlated with surface ozone concentrations in the central valley (e.g., Smith et al. 1984; Smith 1994; Fairley and De Mandel 1996, Ship and McIntosh 1999). The shape of the 500-mb pressure surface at 5500-m elevation. The shape of the 500-mb height contours over the Eastern Pacific is broad and flat and can extend inland for 100s of km.

Accompanying the warm temperatures aloft, are warm temperatures on the central valley floor. Table Bob-8 presents a summer surface climatology for the cities of Redding, Sacramento, San Francisco, Fresno, Santa Maria, and Bakersfield. The coastal cities of San Francisco and Santa Maria have mean daily maximum temperatures in the low- to mid-70s (deg F) while Sacramento averages about 20 F warmer. The northern and southern ends of the Central Valley, represented by Redding and Bakersfield, average an additional 5 F warmer than Sacramento. This heating causes an inland thermal low-pressure trough as evidenced by the lower station pressures at Redding and Bakersfield. The pressure gradient enhances the movement of the thermally-generated sea breeze through the Carquinez Straight, through other gaps in the coastal range to the north and south of the San Francisco (SF) Bay, and even over the coastal range. Pollutants from the SF Bay Area source region are carried with the breeze to receptor regions within the Central Valley. With the abundant sunlight accompanying this fair weather pattern fair weather, the transported pollutants and the Sacramento Valley and San Joaquin Valley emissions cause frequent exceedances of the 1hr and 8hr standards at several sites in the interior of the Central Valley.

This typical scenario is observed on most summer afternoons. For the SF Bay Area, Hayes et al. (1984), in the now-famous “California Surface Wind Climatology,” assign a frequency of 77% to sea breeze conditions matching average surface wind streamlines at 1600 PST with 75% for the Sacramento Valley. However, the high pressure system can migrate with changes in the planetary weather (Rossby wave) pattern. The center of the pressure cell can move ashore, causing a decrease and even a reversal in the mean pressure gradients observed in Table Bob-8 (Lehrman et al. 1994; Pun et al. 1998). The sea breeze is weakened, and its inland extent can become limited, leading to stagnation conditions fostering higher ozone concentrations in many areas. The high can also move east all together, followed by a trough that ventilates the valley. And the high need not always dominate. During summer 1994, Neff et al (1994) found approximately one-third of the days classified as Pacific High Pressure System, one-third to be inland highs, and one-third to be troughs. The air quality impacts of the position and duration of the high are further discussed in Section 2.6.

2.4.2 Major Transport Couples in Central California

In accordance with the 198 California Clean Air Act, the California Air Resources Board has identified transport couples within the state where “transported air pollutants from upwind areas outside a district can cause or contribute to violations of the state ambient air quality standard for ozone in a downwind district.” (CARB, 1989). Since then, CARB has issued triennial assessments of the impacts of transported pollutants on ozone concentrations (CARB, 1990, 1993).

Realizing the limitations of the state of the art in quantifying transport, ARB staff chose to characterize transport as overwhelming, significant, or inconsequential. Operational definitions of these characterizations have been developed (MDAPTC, 1995). Overwhelming transport denotes a situation where an ozone exceedance can occur in the downwind basin due to upwind emissions even in the absence of any downwind emissions. Significant transport means that both upwind and downwind basin pollutants are necessary to cause an exceedance. Inconsequential transport means that downwind emissions alone are sufficient to cause an exceedance with little or no transport of upwind emissions. In identification of transport couples, ARB staff performed analyses using meteorological methods, air quality methods (ARB, 1989, 1990, 1993) and a combination of the two approaches as outlined by Roberts et al. (1992). These methods and others that are relevant to the current study are summarized in Section 3.7.

The following Central California transport couples and their transport characterization are relevant to the CCOS study (ARB, 1993):

- San Francisco Bay Area (SFBA) to Sacramento Valley (SV) – Overwhelming, significant and inconsequential. Hayes et al. 1984 found the sea breeze pattern in the SV with a frequency of 75%, and Roberts et al (1992) characterized impacts in the Upper Sacramento Valley as overwhelming.
- SFBA to San Joaquin Valley (SJV) – Overwhelming, significant and inconsequential. Using air quality methods, Douglas et al. (1991) found that transport from the SFBA affected the northern SJV 37% of the time.
- SFBA to Mountain Counties (MC) – Significant.
- SFBA to North Central Coast (NCC) – Overwhelming and significant.
- SV to SJV– Significant and inconsequential.
- SV to SFBA – Significant and inconsequential. Two possibilities for this infrequent event are discussed in ARB (1989). During stagnation events, or the rare occurrence of the Hayes et al. (1984) northeasterly scenario in the Sacramento Valley (1% frequency at 1600 PST), a north easterly wind brings SV pollutants in the reverse direction through the Carquinez Straight in to the SFBA. A case of this pattern was observed by Stoeckenius et al. (1994) in their comparison of observed wind stream patterns to the Hayes et al. cases. The other scenario of compensation flow is discussed in Section 2.4.3.
- SJV to SV – Significant and inconsequential. The Hayes et al. (1984) southeasterly scenario occurs only 2-3% of the time in the morning hours during summer, but it could transport pollutants, within the SJV from the previous day, into the SV.
- SV to MC – Overwhelming.
- SJV to MC – Overwhelming.
- SJV to South Central Coast (SCC) – Significant and inconsequential.

In addition to these inter-basin transport couples, other source-receptor areas of interest include:

- Intra-basin transport due to nocturnal eddies, i.e., the Fresno eddy within the SJV and the Schultz eddy north of Sacramento in the SV.
- Intra-basin source-receptor couples such as Sacramento-Folsom, Sacramento-Auburn, or Sacramento-Redding and other Upper SV receptor sites.
- California coastal waters to SCC and CC.
- SJV to Great Basin Valleys – Flux estimates of pollutants that escape from the SJV valley as opposed to returning to the valley in downslope flows. Will aid in modeling boundary conditions.
- SJV to Mojave Desert (specifically the MOP site in Mojave, CA.) – Flux estimates of what leaves the SJV valley through Tehachapi Pass. Will aid in modeling boundary conditions. Roberts et al. (1992) have documented transport to Mojave through Tehachapi, and Smith et al. (1997) have demonstrated the correlation between southern SJV and Mojave ozone concentrations.

2.4.3 Meteorological Scenarios Associated with Ozone Exceedances

Several mesoscale flow features in Central California can have significant air quality impacts by transporting or blocking transport of ozone and precursors between the above source-receptor couples.

The Sea Breeze

Differential heating between the land and ocean causes a pressure gradient between the relatively cooler denser air over ocean and the warmer air over the land. The marine air mass comes ashore. However, this heating takes time to occur and may be impeded if a cloud cover prevents direct insolation of the land. A further complication may be provided by any additional surface pressure gradients due to synoptic conditions that can enhance, hinder, or overwhelm this thermal effect. The actual time of onset of a sea breeze can be difficult to forecast with overnight fog or coastal status. Typically, with calm coastal mornings, rush hour pollutants can accumulate in the coastal source region. Then, as the sea breeze is established (often by late-morning, usually by mid-day), maximum ozone production can occur after pollutants leave the coastal areas. It is well-known that maximum ozone occurs downwind of respective source areas (e.g., Livermore downwind of the SF Bay communities.) Studies of sea breeze effects on Central California air quality include that by Stoeckenius et al, (1994), who found an objective classification scheme.

Nocturnal Jets and Eddies

A low-level nocturnal wind maximum can arise as the nocturnal inversion forms and effectively reduces boundary layer friction. Wind friction can be represented (crudely) as a force

that is directly opposed to the wind (termed the "antitriptic wind" by Schaefer and Doswell 1980). The overall direction of flow is determined by the vector balance among horizontal pressure gradient, Coriolis, and frictional forces. However, in the evening, with the establishment of a surface-based nocturnal inversion, the friction is "turned off." The flow is no longer in balance, and there is a component of the pressure gradient force that is directed along the wind, increasing wind speed, which increases the Coriolis force. Since Coriolis is always 90° to the right of the wind (in the northern hemisphere), this means that the wind must veer. In the SJV, the rapidly moving jet (7-30 m/s) may veer toward the western valley but is channeled by the topography and soon encounters the Tehachapi range. Depending on the temperature structure of the valley, the jet may not be able to exit through Tehachapi Pass (~1400 m), as it can during the neutral stability of daytime convective heating. The air is forced to turn north along the Sierra foothills at the southeastern edge of the SJV. Smith et al. (1981) mapped the Fresno eddy with pibal balloons and described an unusual case where it extended as far north as Modesto. During the Southern San Joaquin Ozone Study, Blumenthal et al. (1985) measured the Fresno eddy extending above 900 m AGL about 50% of the time. Neff et al. (1991) have measured the eddy using radar wind profilers during SJVAQS/AUSPEX. The impact of these jets and eddies is to redistribute pollutants within an air basin. The SJV nocturnal jet can bring pollutants from the north SJV to the south overnight. Ozone created in the south SJV can then be redistributed to the central SJV and/or can be transported into layers aloft by the eddy. The Schultz eddy forms from westerly marine air flow in the south SV valley (which may become a jet with the evening boundary layer) impacting the Sierra and turning north. It can redistribute pollutants to Sutter Buttes and points north and east (or west after a half-circulation) of Sacramento (Schultz, 1975; ARB, 1989).

Bifurcation and Convergence Zones

Marine air entering the Sacramento River Delta region from the west has a "choice", SJV to the south or SV to the north. The position of this zone may move north and south based on flow entering the SV from the north or on the infrequent but sometimes observed southerly flow coming up the SJV axis flow. The relative position of the bifurcation zone may affect the proportion of SFBA pollutants transported to each downwind basin. But the dynamics governing the position of the bifurcation zone are currently not well understood. On the other hand, convergence zones can prevent transport between air basins. In the SFBA-NCC couple, pollutants from the south bay communities (e.g., San Jose) are transported by northwesterly winds through the Santa Clara valley to the south. This flow impacts Gilroy and can continue down the Santa Clara Valley to Pinnacles National Monument if the northwesterly winds crossing inland at Moss Landing continue through Pacheco pass without turning north. However, under perhaps subtly different conditions, some of this onshore flow at Moss Landing will turn north, damming the southerly flow coming from Gilroy in the Santa Clara Valley. Another example of the effect of convergence zones on air quality is provided by Blumenthal et al. (1985). They hypothesize that the increase in mixing heights (~200 m higher than in the north SJV) at the southern end of the SJV is due to damming of the northerly flow against the Tehachapi mountains at the south end. Without this damming effect, the mixing levels over Bakersfield, Arvin and Edison would be even lower, and O₃ concentrations may be higher.

Upslope/Downslope Flow

although with a bit different terminology.

Compensation Flow/Re-Entrainment

This proposed mechanism should be distinguished from the observed nocturnal downslope flow. Rather, this mesoscale circulation is a direct result of mass balance and the necessarily simultaneous compensating for mass loss due to upslope flow. In a closed system, there would be a one-to-one correspondence between pollutant flow upslope and pollutant return in a compensation flow. As air was removed from the valley floor, there would be subsidence motion to replace the air, and finally, a compensation flow of air from the top of the Sierra crest would return to replace the vertically descending air. However, the San Joaquin Valley is not a closed system in many ways. Air to replace that removed by slope flows could be come from the relatively clean western boundary, and need not recirculate pollutants at all.

Given a valid emissions inventory, the interplay of these mesoscale features with the synoptic pattern leads to a conceptual model of ozone formation in the study region. It is desirable to objectively classify the wind patterns into distinct scenarios, where the meteorological impacts on air quality are understood in the context of the model, and

2.5 Atmospheric Transformation and Deposition

Much of the difficulty in addressing the ozone problem is related to ozone's complex photochemistry. The rate of O₃ production is a non-linear function of the mixture of VOC and

NO_x in the atmosphere. Depending upon the relative concentration of VOC and NO_x and the specific mix of VOC present, the rate of O₃ formation can be most sensitive to changes in VOC alone or to changes in NO_x alone or to simultaneous changes in both VOC and NO_x. Understanding the response of ozone levels to specific changes in VOC or NO_x emissions is the fundamental prerequisite to developing a cost-effective ozone abatement strategy, and is the principal goal of CCOS.

2.5.1 Ozone Formation

Photochemical production of O₃ in the troposphere was considered to be important only in highly polluted urban regions until the 1970s. It was believed that transport of stratospheric O₃ was the main source of tropospheric O₃ (Junge, 1963). The results of Crutzen (1973), Fishman et al. (1979), for example, show that photochemical production of O₃ from nitrogen oxides and volatile organic compounds is a major source of O₃ in the troposphere (Warneck, 1988). Recent calculations suggest that about 50% of tropospheric O₃ is due to in-situ production (Müller and Brasseur, 1995). At remote sites tropospheric production accounts for observations of O₃ concentrations that are greater than 25 ppb (Derwent and Kay, 1988).

Haagen-Smit (1952) was the first to determine that photochemistry was responsible for the production of O₃ in the highly polluted Los Angeles basin. Air pollution research has determined the overall reaction mechanism for the production of tropospheric ozone. But many important aspects of the organic chemistry are unknown are topics of current research and these uncertainties are discussed below. Figure 2.5-1. Gives an overview of ozone production in the troposphere.

In the troposphere O₃ is produced through the photolysis of nitrogen dioxide to produce ground state oxygen atoms, O(³P), Reaction (1). The ground state oxygen atoms react with molecular oxygen to produce O₃, Reaction (2), (where M is a third body such as N₂ or O₂).



When nitrogen oxides are present, O₃ reacts with NO to reproduce NO₂.



Reactions (1-3) by themselves, in the absence of CO or organic compounds, do not produce O₃ because these reactions only recycle O₃ and NO_x.

O₃ concentrations are determined by the "NO-photostationary state equation", Equation (4).

$$[\text{O}_3] = \frac{J_1[\text{NO}_2]}{k_3[\text{NO}]} \quad (4)$$

where J_1 is the photolysis frequency of Reaction (1), k_3 is the rate constant for Reaction (3), $[\text{NO}_2]$ is the concentration of nitrogen dioxide and $[\text{NO}]$ is the concentration of nitric oxide. Reactions of NO with HO_2 and organic peroxy radicals, produced through the atmospheric degradation of CO or organic compounds, are required to produce ozone. Tropospheric O_3 formation is a highly nonlinear process (i.e. Dodge, 1984; Liu et al., 1987; Lin et al., 1988).

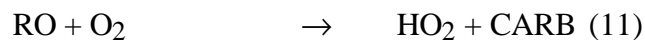
A fraction of O_3 photolyzes to produce an excited oxygen atom, $\text{O}(^1\text{D})$.



A fraction of these react with water to produce HO radicals.



The HO radicals react with CO or organic compounds (RH) to produce peroxy radicals (HO_2 or RO_2). The peroxy radicals react with NO to produce NO_2 which photolyzes to produce additional O_3 :



The net reaction is the sum of Reactions (8) through (12) plus twice Reactions (1) and (2):



where CARB is either a carbonyl species, either an aldehyde ($\text{R}'\text{CHO}$) or a ketone ($\text{R}'\text{CR}''\text{O}$). The carbonyl compounds may further react with HO or they may photolyze to produce additional peroxy radicals that react with NO to produce NO_2 (Seinfeld, 1986; Finlayson-Pitts and Pitts, 1986). Peroxy radical reactions with NO reduce the concentration of NO and increase the concentration of NO_2 . This reduces the rate of Reaction (3) which destroys O_3 and increases the

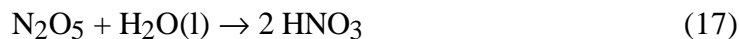
rate of reaction (1) that produces ozone. The increase in the ratio of $[\text{NO}_2] / [\text{NO}]$ leads to higher O_3 concentration according to Equation (4).

Reaction (13) suggests that NO_x is a catalyst for the production of O_3 . The O_3 production efficiency of NO_x can be defined as the ratio of the rate at which NO molecules are converted to NO_2 to the total rate of NO_x lost through conversion to nitric acid, organic nitrates or its loss through deposition (Liu et al., 1987; Lin et al., 1988; Hov, 1989). Under most atmospheric conditions the O_3 production efficiency of NO_x is inversely related to the NO_x concentration.

In the lower troposphere the formation of HNO_3 is a major sink of NO_x because HNO_3 reacts slowly in the lower troposphere and it is rapidly removed due to dry and wet deposition. In the gas-phase NO_2 reacts with HO to form nitric acid by a relatively well understood process.



During the night a significant amount of NO_x can be removed through heterogeneous reactions of N_2O_5 on water coated aerosol particles. Nitrate radical (NO_3) is produced by the reaction of NO_2 with O_3 , Reaction (15). The NO_3 produced may react with NO_2 to produce N_2O_5 , Reaction (16). Finally the N_2O_5 reacts with liquid water to produce HNO_3 , Reaction (17) (DeMore et al., 1997).



The rate of Reaction (17) can be fast during the night-time but its rate constant is very difficult to correctly characterize (Leaith et al., 1988; DeMore et al., 1997). There also may be a gas-phase reaction of N_2O_5 with water but it is relatively small (Mentel et al., 1996).

Uncertainties in rate parameters

The tropospheric chemistry mechanisms are developed using chemical kinetics data from laboratory experiments and these data have uncertainties associated with them. In addition there are difficulties in extrapolating from the laboratory to the real atmosphere. Review panels under the auspices of the International Union of Pure and Applied Chemistry (IUPAC) (Atkinson et al., 1997) and the U.S. National Aeronautics and Space Administration (NASA) (DeMore et al., 1997) evaluate rate constants for use in atmospheric chemistry models. Both groups report not only a recommended value but also uncertainty factors. For example, the NASA review panel gives the nominal rate constants for thermal reactions as:

$$k_o(T) = A \times \exp\left(\left(-\frac{E_a}{R}\right) \times \left(\frac{1}{T}\right)\right) \quad (18)$$

where $k_o(T)$ is the temperature dependent rate constant, A is the Arrhenius factor, R is the gas constant, E_a is the activation energy and T is the temperature (K). The NASA panel assigns an uncertainty factor for 298 K, $f(298)$ and an uncertainty factor for the activation energy, E . Using $f(298)$ and E the NASA panel recommends the following expression for the temperature dependent uncertainty factor:

$$f(T) = f(298) \times \exp\left[\frac{\Delta E}{R} \times \left(\frac{1}{T} - \frac{1}{298}\right)\right] \quad (19)$$

The temperature dependent uncertainty factor is used to calculate the upper and lower bounds to the rate constant:

$$\text{Lower_Bound} = \frac{k_o(T)}{f(T)} \quad (20)$$

$$\text{Upper_Bound} = k_o(T) \times f(T) \quad (21)$$

The upper and lower bounds correspond to approximately one standard deviation:

$$\sigma_k = \frac{k(T) \times f(T) - k(T) / f(T)}{2} \quad (22)$$

However, the upper and lower bounds are not completely symmetric as defined by the NASA panel and the asymmetry becomes more apparent for larger values of $f(T)$ as discussed below.

Rate constants are most accurately known near 298 K and become more uncertain as the temperature becomes lower, for this reason, chemical mechanisms become more uncertain in the upper troposphere. To illustrate this point we calculated the effect of temperature on the uncertainty of rate constants by using the U.S. standard atmosphere (NOAA, 1976). The pressure decreases exponentially with altitude while the temperature decreases with a constant lapse rate with altitude until the tropopause is reached.

Figure 2.5-2 shows the variation of the rate constant with altitude for the reaction of ozone with nitric oxide. The rate constant decreases with increasing altitude due to the temperature decrease. In curve A the upper and lower bounds of the rate constant are shown as dashed lines. The relative uncertainty in the rate constant increases for lower temperatures but the absolute uncertainty decreases for the $O_3 + NO$ reaction. The rate constant for the $CH_3O_2 + HO_2$ reaction is much less well measured than the rate constant for the $O_3 + NO$ reaction, Figure 2.5-3. The uncertainty factor is greater than 2.0 even at 298 K. Both the absolute and the

relative uncertainty increase with altitude for this reaction. For this reaction the NASA recommendations give highly asymmetric error limits. However, the asymmetry is probably more of a defect in the NASA recommendation than a real asymmetry in the uncertainty limits. This is very important because in order to evaluate the combined effect of sensitivities and uncertainties on the reliability of model predictions it is necessary to know the nature of the uncertainty distribution (Thompson and Stewart 1991a,b; Yang et al., 1995; Gao et al., 1995, 1996).

The rate parameters for the reactions of HO radical with many organic compounds have been measured. The rate constant of organic compounds span a wide range of values. If an average HO radical concentration of 7.5×10^6 molecules cm^{-3} is assumed then the atmospheric lifetime of typical organic compounds range from less than an hour to several weeks to over two years for methane, Figure 2.5-4.

Figure 2.5-5 shows nominal rate constants and uncertainty estimates for the reaction of HO with selected alkenes. The uncertainties in these reaction rates are typically ± 20 to 30 % of the recommended value (Atkinson, 1986). The absolute uncertainty is greatest for the most reactive compounds and the rate constants are known best for temperatures near 298 K. More research is needed to better characterize rate constants over a wider range of temperatures.

Uncertainties and deficiencies in atmospheric chemical mechanisms

The chemistry of organic compounds is a major source of uncertainty in the chemical mechanisms. There is a wide variety of organic compounds emitted into the atmosphere, for example Graedel (1979) has inventoried over 350 organic compounds that are emitted from vegetation. In rural and background environments biogenic organic compounds, especially isoprene and terpenes, are often the dominant organic species (Trainer et al., 1987; Chameidies et al., 1988; Blake et al., 1993). Reactive alkenes and aromatic hydrocarbons of anthropogenic origin are often the most important organic precursors of O_3 in urban locations (Leone and Seinfeld, 1985).

Even the predictions of highly detailed explicit mechanisms derived completely from first principles are extremely uncertain because, in spite of extensive recent research [DeMore, 1997; Le Bras, 1997; Atkinson et al., 1997] there is a substantial lack of data. New research, especially on the chemistry of organic compounds, is needed to improve the chemical mechanisms (Gao et al., 1995, 1996; Stockwell et al. 1997). Although the rate constants for the primary reactions of HO, O_3 and NO_3 with many organic compounds have been measured, there have been relatively few product yield studies or studies aimed at understanding the chemistry of the reaction products.

Especially the chemistry of higher molecular weight organic compounds and their photooxidation products is highly uncertain (Gao et al., 1995, 1996; Stockwell et al. 1997). There is little available data on the chemistry of compounds with carbon numbers greater than 3 or 4 and most of the chemistry for these compounds is based upon extrapolating experimental studies of the reactions of lower molecular weight compounds. For example, for alkenes, there is a lack of mechanistic and product yield data even for the reaction of HO with propene. In development of chemical mechanisms it is usually assumed that 65% of the HO radicals add to

the terminal carbon for primary alkenes based upon the work of Cvetanovic (1976) for propene, but there has been little confirmation of these results. For the higher molecular weight alkenes this uncertainty may affect the estimated organic product yields.

The chemistry of intermediate oxidation products including aldehydes, ketones, alcohols, ethers, etc. requires additional study. The nature, yield and fate of most carbonyl products produced from the high molecular weight alkanes, alkenes and other compounds are unknown (Gao et al., 1995, 1996; Stockwell et al. 1997). For photolysis reactions the quantum yields, absorption cross sections and product yields for C4 and higher aldehydes, ketones, alcohols, dicarbonyls, hydroxycarbonyls and ketoacids are not well known. For the reactions of C4 and higher carbonyl compounds with HO and NO₃ the rate constants and product yields need to be measured better.

The reactions of ozone with alkenes and the products are not well characterized (Atkinson, 1994; Stockwell et al. 1997). The fate of Criegee biradicals and their reaction products may be incorrectly described by the mechanisms; especially for any Criegee biradicals beyond those produced from ethene and propene. These uncertainties include the nature and yield of radicals and organic acids. More data are required on the nature of the products of NO₃ - alkene addition reactions. The relative importance of unimolecular decomposition, reaction with oxygen and isomerization reactions of higher alkoxy radicals is unknown and this may affect ozone production rates.

This lack of understanding of alkene chemistry is particularly significant for biogenics like isoprene and terpenes (Stockwell et al. 1997). The photochemical oxidation of biogenic compounds yields a wide variety of organic compounds including peroxyacetyl nitrate (PAN), methyl vinyl ketone, methacrolein and 3-methylfuran, organic aerosols and it may produce additional O₃ if NO_x is present (Paulson et al., 1992a,b). Isoprene and terpenes react rapidly with HO and O₃. The lifetime of isoprene with respect to its reaction with HO is estimated to be 24 minutes and the lifetime of *d*-limonene is about 3.2 hours if the rate constants provided by Atkinson (1994) and an HO concentration of 5 × 10⁶ are used. The terpenes react very rapidly with O₃; α-Pinene and *d*-limonene have a lifetime of 2.2 hours and 54 minutes, respectively, with respect to reaction with O₃ assuming the rate constants of Atkinson (1994) and an O₃ mixing ratio of 60 ppb. Although the outlines of the atmospheric chemistry of isoprene are known much more research is needed before terpene oxidation mechanisms are understood.

The uncertainties in aromatic chemistry are very high (Yang et al., 1995; Gao et al., 1995, 1996; Stockwell et al., 1997). The nature of all the products have not been characterized. The initial fate of the HO - aromatic adduct is not known. Cresol formation, which has been observed by a number of groups, may be an experimental artefact or its formation may occur in the real atmosphere. At some point during the oxidation cycle the aromatic ring breaks but for most aromatic compounds it is not known at what reaction step or ring location. Most operational mechanisms use parameterizations based upon smog chamber data which possibly are inappropriate for the real atmosphere.

The reactions of peroxy radicals (RO₂) are important under night time conditions when nitric oxide concentrations are low. The RO₂ - RO₂ reactions and NO₃ - RO₂ reactions strongly

affect PAN and organic peroxide concentrations through their impact on nighttime chemistry (Stockwell et al., 1995; Kirchner and Stockwell, 1996, 1997). These reactions need to be better characterized.

Photolysis frequencies are also uncertain due to uncertainties in quantum yields, absorption cross sections and actinic flux. The photolysis frequencies of even the most important air pollutants, O₃ and NO₂, remain uncertain because of uncertainties in the measured absorption cross sections and quantum yields. For these compounds the combined uncertainties in the absorption cross sections and quantum yields is between 20 to 30% (Yang et al., 1995; Gao et al., 1995, 1996). Furthermore although the actinic flux is not a direct component of a mechanism, it is important to note that the actinic fluxes used in experimental measurements can be very different than typical atmospheric conditions. Mechanisms based on experiments that used actinic fluxes that are very different from the real atmosphere may incorporate inappropriate chemistry.

Sensitivities, uncertainties and model predictions

Uncertainty estimates given by NASA, IUPAC and other reviews are now being used to determine the reliability of model calculations. There are uncertainties in direct measurements of rate constants and product yields including both systematic and random errors in the data. These uncertainties are easiest to quantify if the measurements have been performed in a number of different laboratories. If there are a reasonable number of experiments, in principle error bounds can be estimated from the experimental standard deviations. The most important problem is that usually there are only a few measurements, the measurements are often of variable quality, and a complete error analysis is not always made of the measurement data. The NASA and IUPAC panel estimates are described as corresponding to $\pm 1\sigma$ but the intention of the reviewers is not always clear. The values are subjectively estimated, and generally not based on detailed statistical analysis. The review panels need to give much greater attention to uncertainty assignments. Improved uncertainty assignments are especially important because uncertainty assignments are now being used for calculations to help determine the reliability of photochemical model predictions as described below.

The sensitivity of chemical concentrations to small variations in rate parameters is one measure (but not the only measure) of the relative importance of a reaction. The direct decoupled method (McCroskey and McRae 1987; Dunker 1984) was used to determine sensitivity coefficients for a continental case (Stockwell et al., 1995). Figure 2.5-6 gives the relative sensitivities of the calculated concentrations of ozone to rate parameters. The concentrations of O₃ are sensitive to the photolysis rates of NO₂, and O₃ because these are important sources of ozone and HO radicals. The concentrations were also very sensitive to the formation and decomposition rates of PAN. The O₃ concentration is sensitive to the rates for the reaction of peroxy radicals with NO and to the reaction rates of HO with CO and organic compounds because these reactions are sources of peroxy radicals. The O₃ concentration is sensitive to the reaction rates of HO₂ with methyl peroxy radical and acetyl peroxy radical (Stockwell et al., 1995).

Gao et al. (1995) calculated local sensitivity coefficients for the concentrations of O₃, HCHO, H₂O₂, PAN, and HNO₃ to the values of 157 rate constants and 126 stoichiometric coefficients of the RADM2 gas-phase mechanism (Stockwell et al., 1990). Gao (1995) found that the RADM2 mechanism exhibits similar sensitivities to input parameters as do other widely used mechanisms (Gery et al., 1989; Carter, 1990). Thus the uncertainty estimates presented for RADM2 mechanism should be generally representative of mechanisms used in current atmospheric chemistry models. Gao et al.'s sensitivity analysis was combined with estimates of the uncertainty in each parameter in the RADM mechanism, to produce a local measure of its contribution to the uncertainty in the outputs. They used several different sets of simulation conditions that represented summertime surface conditions for urban and nonurban areas. The analysis identified the most influential rate parameters to be those for PAN chemistry, formation of HNO₃, and photolysis of HCHO, NO₂, O₃ and products (DCB) of the oxidation of aromatics. Rate parameters for the conversion of NO to NO₂ (such as O₃ + NO, HO₂ + NO, and organic radical + NO), and the product yields of XYLP (organic peroxy radical) in the reaction of xylene + HO and DCB in the reaction XYLP + NO, are also relatively influential.

When Gao et al. (1995) compared the parameters to which ozone is most sensitive to those parameters contributing to the most uncertainty it was found that seven to nine of the same parameters were in "top ten" of both lists for each case examined. However, the rankings of the most influential rate parameters differ between the sensitivity results and the uncertainty results because some parameters are substantially more uncertain than others. Some of the parameters that contribute relatively large uncertainties, e.g., rate parameters for the reactions HO + NO₂ and O₃ + NO, are already well studied, with small uncertainties to which concentrations of some products are highly sensitive.

Monte Carlo calculations examining uncertainties in chemical parameters have been performed previously for descriptions of gas-phase chemistry in the stratosphere (Stolarski *et al.*, 1978; Ehhalt *et al.*, 1979) and clean troposphere (Thompson and Stewart, 1991a,b). Thompson and Stewart used the Monte Carlo method to investigate how uncertainties in the rate coefficients of a 72-reaction mechanism translate into uncertainties in output concentrations of key tropospheric species for conditions representing clean continental air at mid-latitudes. The mechanism studied includes methane, ethane and the oxidation products of these two hydrocarbons. Uncertainties of approximately 20 % and 40 % were found for surface O₃ and H₂O₂ concentrations, respectively, due to the rate uncertainties.

This work was extended by Gao et al. (1996) who performed Monte Carlo analysis with Latin hypercube sampling. Gao et al. showed that the rate parameter for the reaction HO + NO₂ → HNO₃ was highly influential due to its role in removing NO_x and radicals from participation in gas-phase chemistry. The rate parameter for the reaction HCHO + hv → 2HO₂ + CO was highly influential as a source of radicals. Rate parameters for O₃ photolysis and production of HO from O¹D, and parameters for XYLP oxidation were also relatively influential because these reactions were net sources of radicals. Rate parameters for NO₂ photolysis, the reaction of O₃ + NO, and PAN chemistry were substantially more important for absolute ozone concentrations than for responses to reductions in emissions.

Gao et al. (1996) showed that the uncertainties in peak O₃ concentrations predicted with the RADM2 mechanism for 12-hour simulations range from about ±20 to 50%. Relative uncertainties in O₃ are highest for simulations with low initial ratios of reactive organic compounds to NO_x. Uncertainties for predicted concentrations of other key species ranged from 15 to 30% for HNO₃, from 20 to 30% for HCHO, and from 40 to 70% for PAN. Uncertainties in final H₂O₂ concentrations for cases with ratios of reactive organic compounds to NO_x of 24:1 or higher range from 30 to 45%.

Monte Carlo analysis has also been applied to ozone forming potentials and used to quantify their uncertainty. The total O₃ production induced by an organic compound is related to the number of NO-to-NO₂ conversions affected by the compound and its decomposition products over compound's entire degradation cycle. The greater the number of NO-to-NO₂ conversions affected by the compound, the greater the amount of O₃ produced (Leone and Seinfeld, 1985). This ozone formation potential can be quantified as an incremental reactivity, Equation (23).

$$IR_j = \lim_{\Delta HC_j \rightarrow 0} \left[\frac{R(HC_j + \Delta HC_j) - R(HC_j)}{\Delta HC_j} \right] = \frac{R}{HC_j} \quad (23)$$

where R(HC_j) is the maximum value of ([O₃] - [NO]) calculated from a base case simulation and R(HC_j + ΔHC_j) is the maximum value of ([O₃] - [NO]) calculated from a second simulation in which a small amount, ΔHC_j, of an organic compound, j, has been added (Carter and Atkinson, 1989). Maximum incremental reactivities (MIR) are defined as the incremental reactivities for ozone determined under conditions that maximize the overall incremental reactivity of a base organic mixture.

Calculated incremental reactivities are dependent upon simulation conditions and the chemical mechanism used to make the calculations (Chang and Rudy, 1990; Dunker, 1990; Derwent and Jenkin, 1991; Milford et al., 1992; Carter 1994; Yang et al., 1995). Yang et al. (1995) performed calculations with a single-cell trajectory model employing a detailed chemical mechanism (Carter, 1990). They calculated the MIRs for a number of compounds (Yang et al., 1995). Furthermore (Yang et al., 1995) estimated the uncertainty of the mechanism rate parameters and product yields. Monte Carlo calculations were performed to estimate the uncertainty in the incremental reactivities.

Figure 2.5-7 shows MIRs of 26 organic compounds and their uncertainties (1σ) as calculated from Monte Carlo simulations (Yang et al., 1995). The uncertainties ranged from 27% of the mean estimate, for 2-methyl-1-butene, to 68% of the mean, for ethanol. The relatively unreactive compounds tended to have higher uncertainties than more reactive compounds. The impact of the more reactive compounds on O₃ was not affected by small changes in their primary oxidation rates because these compounds reacted completely over the 10-hr simulation period used by Yang et al.

Yang et al. (1995) used regression analysis to identify the rate constants that have the strongest influence on the calculated MIRs. Their results showed that the same rate constants that are influential for predicting O₃ concentrations are also influential for MIRs. For the most of the reactive organic compounds the rate constant for its primary oxidation reaction was influential on the MIR. The rate parameters for the reactions of secondary chemical products were more important for highly reactive compounds because the primary species reacted completely. Compounds that react relatively slowly with HO show a high sensitivity to the uncertainties in the rate of HO production by the photolysis of O₃ photolysis and reactions of O¹D. Rate constants for the reactions of the products are also influential for most compounds. The MIRs for alcohols and olefins were sensitive to uncertainties in the associated aldehyde photolysis rates, and those of aromatics to uncertainties in the photolysis rates of higher molecular weight dicarbonyls and similar aromatic oxidation products (represented by AFG1 and AFG2). Although Yang et al. used a box model, the 3-d simulations by Russell et al. (1995) yielded similar results. The sensitivity analysis by Yang et al. underscores the need to improve the organic component in tropospheric chemistry mechanisms.

Gas-Phase Mechanism Evaluation

Chemical mechanisms need to be evaluated and tested before they are widely used but, unfortunately, there are no generally accepted methods. Ideally field measurements should be used but these are typically limited to only a few species and interpretation is greatly complicated by varying meteorological conditions. Environmental chamber experiments are an alternative approach for the testing condensed chemical mechanisms. Typically the differences between modelled and measured ozone concentrations are about 30%. Better environmental chamber data is required because the data now available suffers from several limitations; these include very high initial concentrations, wall effects and uncertainties in photolysis rates (Stockwell et al., 1990; Kuhn et al., 1997).

Many species are more sensitive to the details of the chemical schemes than ozone and comparisons between models and measurements for these may help in evaluating the mechanisms (Kuhn et al., 1997). For example, routine measurements of both reactive hydrocarbons and carbonyl compounds may provide a data-base which should be valuable for testing model predictions (Solberg et al., 1995). Comparison of measurements and simulation results for H₂O₂ (Slemr and Tremmel, 1994) or nitrogen species can also provide a good test for chemical mechanisms (Stockwell, 1986; Stockwell et al., 1995). Given that differences in the carbonyl predictions of different chemical mechanisms are often larger than a factor of two, such measurements are much more useful than ozone in discriminating between mechanisms (Kuhn et al., 1997).

The intercomparison of field measurements and model simulations for HO can be used to test the fast photochemistry in the troposphere. Model simulations for HO are only slightly affected by transport, since the lifetime of HO is in the order of a few seconds. Therefore the concentration of HO is determined by the concentrations of the precursors. Poppe et al (1994) presented a comparison between model simulations based on the RADM2 chemical mechanism (Stockwell et al., 1990) and measurements for rural and moderately polluted sites in Germany. They showed that the measured and modeled HO concentrations for rural environments correlate well with a coefficient of correlation $r=0.73$ while the model over predicts HO by about 20%.

Under more polluted conditions the correlation coefficient between experimental and modeled data is significantly smaller ($r=0.61$) and the model over predicts HO by about 15%. Poppe et al. (1994) concluded that the deviations between model simulations and measurements are well within the systematic uncertainties of the measured and calculated HO due to uncertain rate constants. In contrast to these results McKeen et al. (1997) failed to simulate measured concentrations of HO with a photochemical model. Their model consistently over predicted observed HO from the Tropospheric OH Photochemistry Experiment (TOHPE) by about 50%.

Agreement between the gas-phase mechanisms

The intercomparison of chemical mechanisms is one way to assess the degree of consensus among the mechanism builders. A decision about which chemical mechanism performs the best cannot be made on the basis of model intercomparisons and the fact that a model produces results in the central range of the other models is not a proof of correctness (Dodge, 1989). Only comparisons with real measurements made in the atmosphere provide the final assessment of the performance of a chemical mechanism (Kuhn et al., 1997).

Olson et al. (1997) and Kuhn et al. (1997) compared the predictions of gas-phase chemical mechanisms now in wide use in atmospheric chemistry models. The Intergovernmental Panel on Climate Change (IPCC) compared simulations made with several chemical schemes used in global modeling in a study named PhotoComp (Olson et al., 1997). In PhotoComp each participant used their own photolysis frequencies. Many of the differences between the simulations made with the mechanisms could be attributed to differences in photolysis frequencies, especially for O₃, NO₂, HCHO and H₂O₂. The mechanisms predicted different HO₂ concentrations and these differences were attributed to inconsistencies in the rate constants for the conversion of HO₂ to H₂O₂ and differences in the photolysis rates of HCHO and H₂O₂ (Olson et al., 1997).

The intercomparison by Kuhn et al. (1997) extended the IPCC exercise to more polluted scenarios that are more typical for the regional scale. The cases used in this study were a representative set of atmospheric conditions for regional scale atmospheric modeling over Europe. In contrast to PhotoComp, the most polluted case included emissions. Photolysis frequencies were prescribed for the study of Kuhn et al. (1997) to ensure that the differences in results from different mechanisms are due to gas phase chemistry rather than radiative transfer modeling.

Most of chemical mechanisms yielded similar O₃ concentrations (Kuhn et al., 1997). This is not unexpected, since many of the schemes were designed to model ozone and therefore were selected for their ability to model the results of environmental chamber experiments. However, looking at the deviation of the tendencies rather than the final concentrations, the differences were substantial: these ranged from 15 to 38% depending upon the conditions. For the HO radical the noon time differences between mechanisms ranged from 10 to 19% and for the NO₃ radical the night time differences ranged from 16 to 40%. Calculated concentrations of other longer-lived species like H₂O₂ and PAN differed considerably between the mechanisms. For H₂O₂ the rms errors of the tendencies ranged from 30 to 76%. This confirms earlier findings by Stockwell (1986), Hough (1988) and Dodge (1989). The differences in H₂O₂ can partly be

explained by the incorrect use of the HO_2+HO_2 rate constant (Stockwell, 1995) and by differences in the treatment of the peroxy radical interactions. Large differences between mechanisms are observed for higher organic peroxides and higher aldehydes with a rms error of around 50% for the final concentration in the most polluted case.

2.5.2 Heterogeneous Reactions and Ozone - Secondary Aerosol Formation

Reactions occurring on aerosol particles or in cloud water droplets may have a large affect on the constituents of the troposphere (Baker, 1997; Andreae and Crutzen, 1997; Ravishankara, 1997). Heterogeneous reactions may be defined as those reactions that occur on the surfaces of solid aerosol particles while multiphase reactions are reactions that occur in a bulk liquid such as cloud water or water coated aerosol particles (Ravishankara, 1997). Particles may affect gas-phase tropospheric concentrations through both chemical and physical processes. Sedimentation of aerosol particles or rain out removes soluble species from the gas-phase leaving behind the relatively insoluble species. Cloud water or water coated aerosols may scavenge soluble reactive species such as HO_2 , acetyl peroxy radicals, H_2O_2 and HCHO (Jacob 1986; Mozurkewich et al. 1987). Ozone formation is suppressed by the removal of HO_2 radicals and highly reactive stable species such as HCHO.

The loss of HO_2 and H_2O_2 influences the hydrogen cycle in the gas phase (Jacob 1986) and furthermore HO_2 is lost in the liquid phase through its reactions with copper ions, ozone and by its self reaction (Walcek et al., 1996). These effects reduce the concentrations of HO and HO_2 radicals in clouds. Jacob (1986) estimated a decrease of approximate 25% while Lelieveld and Crutzen (1991) estimated a decrease of 20 to 90% although Lelieveld and Crutzen's gas-phase chemical mechanism would be expected to over estimate gas-phase HO_2 concentrations in clear air (Stockwell, 1994). The reduction of HO_x concentrations reduced ozone concentrations (Lelieveld and Crutzen 1991). In relatively clean areas with NO_x concentrations smaller than 100 ppt, the ozone destruction rate is increased by clouds by a factor of 1.7 to 3.7 (Lelieveld and Crutzen, 1991). Jonson and Isaksen (1993) also found that the clouds are most effective in reducing ozone concentrations under clean conditions and they calculated a reduction between 10 and 30% for clean conditions.

Lelieveld and Crutzen (1991) and Jonson and Isaksen (1993) did not consider the effects of the reactions of dissolved transition metals in their calculations. If models include reactions involving copper, iron and manganese a different result is obtained. The ozone destruction rate is decreased by clouds by 45 to 70% for clean conditions (Matthijsen et al. 1995, Walcek et al. 1996). In polluted areas with high NO_x concentration the photochemical formation rate of ozone is also decreased. Lelieveld and Crutzen (1991) found a decrease in the photochemical formation rate of ozone by 40 to 50% and Walcek et al. (1996) found a decrease by 30 to 90%. Matthijsen et al. (1995) came to the result that the reaction between Fe(II) and ozone was especially important and it increases the ozone destruction rate in polluted areas by a factor of 2 to 20 depending on the iron concentration. Peroxy acetyl nitrate (PAN) concentrations may be converted to NO_x through the scavenging of acetyl peroxy radicals by cloud water even though PAN itself is not very soluble (Villalta et al., 1996). This process would tend to increase ozone concentrations.

Heterogeneous, multiphase and gas-phase reactions may have comparable effects on the concentrations of tropospheric species (Ravishankara, 1997). Although heterogeneous and multiphase reactions typically affect the same species as gas-phase reactions the overall result may be very different. Sulfur dioxide may be oxidized to sulfate by all three reaction types but only the gas-phase oxidation of SO_2 leads to the production of new particles.

Tropospheric multiphase reactions have received recent attention because of their role in tropospheric acid deposition (Calvert, 1984) and more recently in stratospheric ozone depletion (WMO, 1994). Aqueous phase reactions occurring in cloud water are very important examples of multiphase reactions. Many theoretical studies suggest that clouds affect tropospheric chemistry on the global scale (Chameides, 1986; Crutzen, 1996; Chameides and Davis, 1982; Chameides, 1984; Chameides and Stelson, 1992). Clouds cover more than 50% of the Earth's surface and occupy about 7% of the volume of the troposphere under average conditions (Pruppacher and Jaenicke, 1995; Ravishankara, 1997). Clouds strongly affect the actinic flux reaching reactive species. Depending upon conditions and location in the atmosphere, clouds can increase or decrease actinic flux (Madronich, 1987). Photolysis rates within droplets may be high because of multiple reflections. The conversion of SO_2 to sulfate by H_2O_2 or O_3 in cloud water is an important example of a multiphase chemical process (Penkett et al., 1979; Gervat et al., 1988; Chandler et al., 1988). Another potentially important process is suggested by recent studies that show that the photolysis of rainwater containing dissolved organic compounds may produce H_2O_2 at a rapid rate (Gunz and Hoffmann, 1990; Faust, 1994).

Many multiphase reactions may be much faster than their corresponding gas-phase counterparts. The most important multiphase reactant is often water and many hydrolysis reactions have a somewhat heterogeneous character because the reactions are so fast that they are completed at or very near to the water surface (Hanson and Ravishankara, 1994). N_2O_5 rapidly hydrolyzes in the presence of liquid water but this reaction is extremely slow in the gas-phase (W. B. DeMore et al., 1997). The oxidation of SO_2 by H_2O_2 in cloud water is very fast but it does not occur in the gas-phase (Calvert and Stockwell, 1984). Even very slow hydrolysis reactions may be the dominate reactions because of overwhelming water concentrations. Other multiphase reactions will be important only if hydrolysis is extremely slow (Ravishankara, 1997).

There is often no gas-phase counterpart to the aqueous-phase reaction. Tropospheric sulfate aerosol may participate in many multiphase reactions that are acid catalyzed. Sulfate aerosols may reduce HNO_3 to NO_x through reactions involving aldehydes, alcohols and biogenic emissions and they may convert CH_3OH to CH_3ONO_2 making sulfate aerosol the dominate source of CH_3ONO_2 in the troposphere (Tolbert et al., 1993; Chatfield, 1994; Ravishankara 1997).

Gas-phase sources of halides in the troposphere are small and on a global basis sea-salt aerosols are a major source. Halogens are strong oxidants, they may affect ozone concentrations in the Arctic and are therefore potentially very important (Barrie et al., 1988). The marine boundary contains large numbers of sea-salt aerosols that contain high concentrations of halides. Halides and their compounds may be released from the sea-salt aerosols through the scavenging and reactions of compounds such as NO_3 , N_2O_5 and HOBr (Finlayson-Pitts et al., 1989; Vogt et

al., 1996; Ravishankara, 1997). The water content of the sea-salt aerosol may be an important variable for characterizing the chemistry of these aerosols because they may react differently if they are above the deliquescence point than if they are below (Rood et al., 1987, Ravishankara 1997).

Multiphase reactions involving organic compounds may be important as mentioned above. The characteristics of organic containing aerosols are not well known but they are formed from emissions of organic compounds from biogenic and anthropogenic sources (Mazurek et al., 1991; Odum et al., 1997). The oxidation of organic compounds leads to the production of a wide variety of highly oxygenated compounds including, aldehydes, ketones, dicarbonyls and alcohols that are condensable or water soluble. For example, in rural regions biogenically emitted organics such as α -pinene react with ozone produce aerosols (Finlayson-Pitts and Pitts, 1986) and in urban areas the photochemical oxidation of gasoline may be an important organic continuing aerosol source (Odum et al., 1997).

Examples of important heterogeneous reactions include those occurring on ice, wind blown dust, fly ash and soot. Heterogeneous reactions on cirrus clouds involving ice, N_2O_5 and other species may be important in the upper troposphere. These reactions could remove reactive nitrogen from the upper troposphere. These processes could play an important role in determining the impact of aircraft on this part of the atmosphere (Ravishankara, 1997).

Fly ash and wind blown dust typically contain silicates and metals such as Al, Fe, Mn and Cu (Ramsden and Shibaoka, 1982; Ravishankara 1997). Photochemically induced catalysis may oxidize SO_2 to sulfate or produce oxidants such as H_2O_2 (Gunz and Hoffmann, 1990). On the other hand, soot contains mostly carbon and trace substances. The understanding of soot is a very important because it may affect the Earth's radiation balance through its strong radiation absorbing properties. Soot may reduce HNO_3 to NO_x and otherwise react as a reducing agent (Hauglustaine et al., 1996; Rogaski et al., 1997; Lary et al., 1997). It is difficult to estimate the importance of heterogeneous reactions because changes to the aerosol's surface will strongly affect its chemical properties. For example, the surface of soot particles may become oxidized or coated by condensable species (Ravishankara 1997).

Multiphase reactions are better understood than heterogeneous reactions but in neither case is the understanding satisfactory. Unfortunately particle microphysics is insufficiently well understood to estimate the rates of heterogeneous and multiphase reactions with an accuracy similar to the gas-phase (Baker, 1997; Ravishankara, 1997). These required particle characteristics may include surface area, volume, composition, phase, Henry's law coefficients, accommodation coefficients and reaction probabilities, depending upon the reaction.

For many atmospheric chemistry modeling applications it would be adequate to consider the gas-phase chemistry as primary and to represent the effect of heterogeneous and multiphase reactions as first order loss reactions of gas-phase species (Ravishankara 1997). Walcek et al. (1996) have used this general approach to couple gas and aqueous-phase chemistry mechanisms. One approach to multiphase reaction rates is to calculate them from a knowledge of mass transport rates, diffusion constants, solubilities and liquid-phase reaction rate constants and correct them to apply to small atmospheric droplets (Danckwerts, 1951, 1970; Schwartz, 1986).

Alternatively, another approach for describing the overall reactive uptake coefficients of gas-phase species for multiphase reactions is to treat them as a network of resistances as has been done for the stratosphere (Hanson et al., 1994, Kolb et al.; 1995). This same approach may be applied to tropospheric multiphase reactions (Ravishankara, 1997). The first resistance is due to diffusion of molecules through the gas-phase to a droplet surface. The mass transfer rate is calculated from the equations of Fuchs and Sutugin (1970; 1971) and the droplet size spectrum. The transfer of a molecule from the gas-phase to the liquid-phase is the second resistance. The probability of this process is described by a mass accommodation coefficient (Ravishankara, 1997). Once the molecule enters the liquid-phase it must diffuse through the liquid before it reacts. The liquid-phase reaction rate is described by a rate coefficient. More measurements of mass accommodation coefficients or the means to reliably calculate them for many species are required along with measurements of liquid-phase reaction rate constants. The methods of Hanson et al. (1994) and by Schwartz (1986) provide the same results but the approach of Schwartz may be more convenient to use for clouds while the approach of Hanson et al. may be easier to use for fine particles.

The mechanisms of heterogeneous reactions are too poorly known to produce anything like the schemes for multiphase reactions described above. The mechanisms for surface diffusion and dissociation are unknown (Ravishankara, 1997). Heterogeneous reaction rates are typically more sensitive than multiphase reactions to the mass transfer to a surface and therefore these rates are more dependent on the total surface area. Heterogeneous reactions may be more or less important in the troposphere than in the stratosphere depending on whether the reactants are physisorbed or chemisorbed on to the solid surface. Heterogeneous reactions involving two molecules physisorbed on to a solid surface would be expected to be much slower due to the greater temperatures in the troposphere but the reaction rate of species that are chemisorbed on a surface are probably not as sensitive to temperature (Ravishankara, 1997). If there is some energy barrier to the scavenging of one of the reactants, such as dissociation on the particle surface, than the heterogeneous reaction rate may even increase with temperature. However if water is a reactant, the rate of a heterogeneous reaction may be more sensitive to the relative humidity than temperature.

Determination of the chemical and microphysical parameters required to estimate the effect of heterogeneous and multiphase reactions should be a research priority. However, field measurements of the composition, surface characteristics, phase, number, size spectra, time trends and other characteristics of atmospheric particles may be even more important. Field measurements may provide the most reliable assessment of the rates and relative importance of heterogeneous and multiphase reactions in the troposphere during the next few years. (Ravishankara, 1997).

2.5.3 Role of Ozone Precursors from Natural Sources

A variety of organic compounds are emitted by vegetation. Most biogenic compounds are either alkenes or cycloalkenes. Because of the presence of carbon double bond, these molecules are susceptible to attack by O_3 and NO_3 , in addition to reaction with OH radicals. The atmospheric lifetimes of biogenic hydrocarbons are relatively short compared to those of

other organic species. The OH radical and ozone reactions are of comparable importance during the day, and the NO₃ radical reaction is more important at night.

Isoprene is generally the most abundant biogenic hydrocarbon except where conifers are the dominant plant species. Isoprene reacts with OH radical, NO₃ radicals, and O₃. The OH-isoprene reaction proceeds almost entirely by the addition of OH radical to the C=C double bond. Formaldehyde, methacrolein, and methyl vinyl ketone are the major products of the OH-isoprene reaction.

The O₃-isoprene reaction proceeds by initial addition of O₃ to the C=C double bonds to form two primary ozonides, each of which decomposes to two sets of carbonyl plus biradical products. Formaldehyde, methacrolein, and methyl vinyl ketone are the major products of the O₃-isoprene reaction.

2.5.4 Relative Effectiveness of VOC and NO_x Controls

The relative behavior of VOCs and NO_x in ozone formation can be understood in terms of competition for the hydroxyl radical. When the instantaneous VOC-to-NO₂ ratio is less than about 5.5:1, OH reacts predominantly with NO₂, removing radicals and retarding O₃ formation. Under these conditions, a decrease in NO_x concentration favors O₃ formation. At a sufficiently low concentration of NO_x, or a sufficiently high VOC-to-NO₂ ratio, a further decrease in NO_x favor peroxy-peroxy reactions, which retard O₃ formation by removing free radicals from the system.

In general, increasing VOC produces more ozone. Increasing NO_x may lead to either more or less ozone depending on the prevailing VOC/NO_x ratio. At a given level of VOC, there exists a NO_x mixing ratio, at which a maximum amount of ozone is produced, an optimum VOC/NO_x ratio. For ratios less than this optimum ratio, increasing NO_x decreases ozone. This situation occurs more commonly in urban centers and in plumes immediately downwind of NO sources. Rural environments tend to have high VOC/NO_x ratios because of the relatively rapid removal of NO_x compared to that of VOCs.

2.5.5 Atmospheric Deposition

Dry deposition is the transport of gaseous and particulate species from the atmosphere onto surfaces in the absence of precipitation. The factors that govern the dry deposition of a gaseous species or particle are the level of atmospheric turbulence, the chemical properties of the depositing species, and the nature of the surface itself. The level of turbulence in the atmosphere governs the rate at which species are delivered down to the surface. For gases, solubility and chemical reactivity may affect uptake at the surface. The surface itself is a factor in dry deposition. A non-reactive surface may not permit absorption or adsorption of certain gases; a smooth surface may lead to particle bounce-off. Natural surfaces, such as vegetation generally promote dry deposition.

Eddy correlation is the most direct micrometeorological technique. In this technique, the vertical flux of an atmospheric trace constituent is represented by the covariance of the vertical

velocity and the trace constituent concentration. Fluxes are determined by measuring the vertical wind velocity with respect to the Earth and appropriate scalar quantities (gas concentrations, temperature, etc). These measurements can be combined over a period of time at a single location (such as measurements made at a stationary location from a tower) or over a wide area (as with measurements made with aircraft) to yield a better understanding of the role surface characteristics, such as vegetation, play in the exchange of mass, momentum, and energy at the Earth's surface.

2.6 Conceptual Model of Ozone Episodes and Transport Scenarios of Interest

This section starts with a brief summary of the current conceptual model as documented by Pun et al. (1998). Modifications to the model are introduced with discussion of a possible link between coastal meteorology, specifically fog formation) and central valley air quality, possible applications to air quality forecasting.

The search for an objective classification scheme, consistent with past studies and with the classification scheme of Hayes et al. (1984), is discussed. A preliminary subjective analysis of synoptic weather for ozone seasons 1996-98 is presented, with the intent to develop an objective classification scheme of common scenarios.

2.6.1 Current Conceptual Model of Ozone Formation and Transport

During a typical summer day, airflow over the Pacific Ocean is dominated by the Eastern Pacific High-Pressure System (EPHPS). Off the coast of central California, outflow from the anticyclone becomes westerly and penetrates the Central Valley through various gaps along the coastal ranges. The largest gap in the coastal ranges is located in the San Francisco Bay Area. Airflow reaching the Central Valley through the Carquinez Straits is directed Northward into the Sacramento Valley, southward into the San Joaquin Valley (SJV), and eastward into the Mountain Counties. The amount of air entering into these regions and the north-south bifurcation of the flow depends on the location, extent, and strength of the EPHPS and on the surface weather pattern. As the low-level divergence from the EPHPS continues to rotate in the clockwise direction, the high can migrate with the planetary wave pattern from west to east. If the EPHPS is approaching the coast of California, it will reinforce on-shore surface gradients and increase the amount of air entering the Sacramento Valley. However, if the center of the EPHPS comes on-shore over central California, the normal surface gradient is diminished and (or can even be reversed). The amount of air entering the Central Valley is reduced. If the southern end of the EPHPS is over the Delta region, the amount of air entering the Central Valley will be blocked, and, in rare cases may even reverse direction through the Carquinez Straits (summer frequency of northeasterly pattern is ~1%, according to Hayes et al. 1984).

This complex feature of airflow, unique to a region from the Pacific Ocean to the Sierra Nevada, and from Yuba City to Modesto, contributes to various types of ozone episodes in the SJV, Sacramento Valley, Mountain Counties and the Bay Area. Both local and transport ozone episodes are observed in the SJV as well as the Sacramento area depending upon the nature of the airflow in the region. In the Bay Area, ozone concentrations are elevated when airflow from

the Bay Area to the Central Valley is limited. Elevated ozone concentrations are observed in the Mountain Counties due mostly to transported pollutants. Transport of pollutants from the northern SJV to the central and southern SJV is accelerated at night due to the “low-level jet” (an airflow that develops at night and moves from the north to south along the SJV with speeds of 10-15 m/sec). Air also rotates in the counterclockwise direction around Fresno (Fresno Eddy) in the morning hours, limiting the ventilation of air out of the SJV. During the day, pollutants are transported from the SJV to the Mojave Desert via the Tehachapi Pass. Occasionally, an outflow from the SJV to the San Luis Obispo area is observed.

The above conceptual model is an oversimplification, but it purports to describe the typical summer pattern. The movement of the EPHPS on-shore often corresponds to the 2-3 day ozone episodes bringing some of the worst air quality to the Central Valley. Meteorologists forecasting coastal fog have studied these semi-cyclic phases. After a brief overview, following the summary of Rogers et al. (1995), a possible link with air pollution meteorology is discussed.

Coastal Meteorology

Coastal meteorology directly influences the mesoscale from about 100 km offshore to 100 km inland (Rogers et al. 1995, concise overview article). The coastal zone includes interaction of the marine and land atmospheric boundary layers, air-sea thermal exchange, and large-scale atmospheric dynamics linked to fog formation by Leipper (1994, 1995) and others as summarized by Leipper (1994). The atmospheric physics of the sea breeze, discussed in Section 2.4, is well understood, but there is currently better understanding of a homogeneous layer, marine layer out at sea or a convective boundary layer over land, than for all the effects of the land-sea interface. The implications for inland air quality are complicated by the inherent variability in a boundary layer depth which can vary from 100--200 m at the shore to several kilometers inland (McElroy and Smith, 1991). Nevertheless, coastal meteorology has significant impacts on inland air quality.

For example, major ozone episodes in the vicinity of Santa Barbara, California are often associated with the storage of ozone precursors in the shallow marine layer over the Santa Barbara Channel (Moore et al. 1991) and the onshore flow of marine air as a miniature cold front (McElroy and Smith 1991). A coherent marine layer, with an imbedded thermal internal boundary layer that forms at the shoreline, can propagate inland for distances of 20 to 50 km.

In addition to the heterogeneity of the coastal zone, the California coastal environment is modified by considerable coastal topography, which can accelerate the wind while constraining the flow parallel to the coast. Rogers et al. (1995) describe the problem as characterized by two free parameters:

- the Froude number Fr , defined by $U/(Nh)$, and
- the Rossby number Ro , defined by $U/(fl)$,

where U is the speed of the air stream, h is the height of the barrier, f is the Coriolis parameter, l is the half width of the barrier, and N is the Brunt-Vaisala frequency of oscillation of gravity waves. Generally blocking of the air flow occurs when Fr is < 1 which can occur with elevations

as low as 100 m. Thus, localized regions of high or low pressure generated in the coastal zone can become trapped and propagate along the coastline for days. These features may have length scales of 1000 km in the alongshore direction and 100-300 km across-shore and can cause significant changes in the local weather in the coastal zone. For example, a southerly surge is defined as the advection of a narrow band of stratus northward along the coast, with a rapid transition from northerly to southerly flow at coastal buoys. It can replace clear skies with clouds and fog, and cause intensification and reversals of the wind field (e.g., Dorman, 1985, 1987; Mass and Albright, 1987). It typically covers 500-1000 km of coastline, propagates at an average speed of 7-9 m/s, and lasts 24-36 hours (Archer and Reynolds, 1996).

However, every summer, southerly winds develop along the coast one or two times a month that are related to synoptic scale flow. The transition from northerly to southerly winds often corresponds to the end of a coastal heat wave and the abrupt onset of stratus. Leipper (1994, 1995) has documented a cycle in coastal fog, with periodic clearing of large areas of clouds off the coast of as warm, offshore flow spread out over the ocean. Leipper (and Kloesel, 1992) have shown that synoptic-to-mesoscale clearing episodes are correlated with ridging of the Pacific subtropical anticyclone in the United States Pacific Northwest region that results in these offshore flows.

Leipper (1994) has identified four phases of fog formation:

- Phase 1: Initial conditions
- Phase 2: Fog Formation
- Phase 3: Fog Growth and Extension
- Phase 4: Stratus

Furthermore, Leipper (1995) has linked the four phases to properties of the Oakland soundings called Leipper Inversion Based Statistics (LIBS). These parameters include the 850-mb temperature and the height of inversion base and top, thickness of the inversion layer, and strength of the inversion, which have been employed by the previously summarized studies. But Leipper also separates the inversion into sublayers of 0-250m, 250-400 m and 400-800 m and looks at wind statistics of these layers and wind direction. He has developed frequency distribution charts, one per phase per U.S. west coast city, linking fog local climatology measures of frequency and intensity (visibility-based) to the four synoptic phases. Such an approach should be investigated for possible applications to Central California ozone forecasting. There may also be a connection in the phases of fog formation to air quality, with an approximate 90° lag in the fog phase relative to the air quality climatology phase.

The use of LIBS in cluster analysis is in-progress. It is planned to discuss and develop these ideas with the Meteorological Working Group and complete inclusion of relevant LIBS parameters in the objective classification of meteorological scenarios with the CCOS Operational Plan.

Previous classification studies

Previous studies have classified California weather and wind flow patterns. Objective classification is possible for air quality in the San Joaquin Valley as the studies summarized below demonstrate.

Hayes et al (1984)

Grouped surface wind patterns for SF Bay Area (6 primary scenarios), San Joaquin Valley (4 primary scenarios), and Sacramento Valley (8 primary scenarios). This document is cited in many of the documents in the included review.

Fairley and DeMandel (1996)

Performed cluster analysis to group ozone episode days ($[O_3] \geq 15$ pphm) for 1985-89. For each cluster, the average peak ozone level in the San Joaquin Valley exceeds 120 ppb.

- Cluster 1: high in San Joaquin Valley, low-moderate in Sacramento Valley, and low in Bay Area
- Cluster 2: high in San Joaquin Valley, moderate in Sacramento Valley, and moderate in Bay Area
- Cluster 3: high in northern San Joaquin Valley, high in Sacramento Valley, and moderate Bay Area
- Cluster 4: high in Bay Area, varies over other areas.

Performed CART analysis on 31 surface and upper-air variables to determine which variables best distinguish between episode and non-episode days:

- Stockton daily maximum temperature
- 900 mb temperature from the 00Z (1600 PST) Oakland sounding

and between clusters:

- Sacramento daily maximum temperature
- v-component (north-south) of Sacramento afternoon winds
- product of Pittsburg 1500 PST u-component (east-west) wind with Oakland inversion base height from the 00Z (1600 PST) sounding

Meteorological features of clusters are identified and discussed, but “ozone levels within clusters vary considerably and . . . clusters could only roughly be predicted with the meteorological variables.” Noted that Cluster 4 days are not characterized by a SARMAP intensive, as with other clusters.

Roberts, P.T., C.G. Lindsey, and T.B. Smith. (1994)

For 1981-89 ozone exceedance days, performed individual and multiple linear regressions between ozone and various meteorological parameters:

- 850-mb and 950-mb temperatures, and inversion height from the 00Z (1600 PST) Oakland sounding
- Daily maximum temperatures from Bakersfield, Fresno, and Modesto
- 12Z (0400 PST) surface pressure gradients from San Francisco to Reno and from San Francisco to Las Vegas

Performed a cluster analysis between Fresno ozone and these meteorological parameters. Estimated mean meteorological parameters on ozone exceedance days. Results are presented in tabular form. Clusters are not specifically identified nor definitively associated with surface flow patterns. One cluster is discussed for which a trough can pass through the northern SJV (and presumably the Sacramento Valley) without materially affecting the southern SJV.

Used paired-station correlations for ozone, Pittsburg v. Bethel Island, and Bethel Island v. Stockton, to follow the transport route west from SF Bay Area (Pittsburg to Bethel Island) and into the San Joaquin Valley (Bethel Island to Stockton).

More detail is available in Roberts et al (1990).

T.B. Smith (1994)

Defined two criteria based on Fresno and Edison maximum ozone concentrations:

- Stringent criteria - O₃>130 ppb at both sites on at least 1 of 2 consecutive days with one of the two sites >140 ppb
- Marginal criteria - O₃>130 ppb at either site on 2 consecutive days but with no value >130 ppb at the other site.

Stringent criteria days were then subjected to a cluster analysis. Two clusters were found that did not differ in main synoptic characteristics, but only by the intensity or development of the synoptic pattern.

Meteorological scenarios associated with SJV episodes include:

- Warm temperature aloft
- Offshore surface pressure gradients (From Reno to SF)
- High maximum temperatures in SJV
- Extensive high-pressure in the western U.S. centered near Four Corners
- Western edge of high should extend to the west coast
- Low pressure trough off-shore
- Southerly winds aloft prevalent along the west coast

Ludwig, Jiang, and Chen (1995)

Performed cluster and empirical orthogonal function (EOF) analysis for ozone violation in Pinnacles national Monument. Found that Pinnacles is often located within the subsidence inversion of the EPHPS. Did not conclude the source region of pollutants or the mechanism responsible for trapping pollutants in the inversion.

Stoeckenius, Roberts, and Chinkin (1994)

Performed streamline analysis and matching of patterns to the Hayes et al. Surface flow patterns. Backtrajectories and forward trajectories were also computed and examined. Generated six source-receptor scenarios with an additional six classifications to describe coastal winds. The main scenarios are:

- Northwest
- Northeast
- Bay Outflow
- Calm
- Southerly
- Northwest-South

They performed a cluster analysis with 17 meteorological variables, and were able to approximately match the Hayes et al. flow patterns. Concluded with an 85% success rate in “forecasting” observed ozone exceedances, but found that four variables were almost as successful. Condition for potential ozone days are:

- Oakland 850-mb temperature ≥ 17.5 °C
- Sacramento and Fresno surface temperature ≥ 85 °F
- San Francisco to Reno sea-level surface pressure difference ≤ 10 mb

Preliminary Subjective Analysis: Inspection of Daily Weather Maps

Table 4.6-1 shows a straw-man synoptic classification scheme for all ozone season days. Visual inspection of 552 days spanning May-October 1996-98 was performed and each day was classified as one of the overall eight types and up to four different subtypes. Ozone impacts by Basin and proposed Sub-basin are qualitatively described as High, Medium and Low. It is possible to define these three impact levels in terms of frequency/probability of occurrence of 8hr and or 1hr exceedance and severity of maximum and/or mean ozone concentration. It is intended to link this top down approach with previous cluster analysis, in particular that of Stoeckenius et al. (1994), and to Hayes et al (1984) surface wind climatology. It is also proposed

to develop this objective classification scheme with ARB and district meteorologists as part of a Meteorology Working Group.

In addition, as part of the proposed meteorological scenarios, the proposed working group should include empirical techniques to assess the frequency of formation, the link to the synoptic patterns, and the air quality impacts of the following mesoscale features:

- SJV/SV Bifurcation Zone – location and relative proportions of air moving north, east, and south. (see section 2.4)
- Pacheco Anti-Cyclone – impact on SJV to San Louis Obispo area.
- Fresno Eddy – degree to which pollutants are trapped and re-entrained in central SJV.
- Schultz Eddy – impacts of transport to northern mountain counties and upper SV
- Redding Eddy – Discuss any evidence for and or possible importance of to Redding area.
- Upper/Lower SV Convergence zone
- Upper/Lower SJV Convergence zone
- Upslope/Downslope (see section 2.4)
- Compensation Flow/Re-entrainment (see section 2.4)
- Coastal Windflow (see section 2.4)
- Marine fog and stratus

Objective cluster analysis is in progress, and, using input from the Meteorology Working Group, to arrive at objectively classified scenarios linked to upper level flow, the “phase” of the synoptic cycle, surface flow, and ultimately the spatial and temporal pattern of ozone concentrations in Central California. This work is planned to be complete for the CCOS Operational Plan

2.6.2 Implications of Change in Federal Ozone Standard on Conceptual Model

Retrospective analysis of the O₃ data for northern and central California during the 1990's show larger downward trends in 1-hour-average peak O₃ concentrations than in 8-hour averages. The implication of the state 1-hour ozone standard and the new federal 8-hour ozone standard is that they require a reappraisal of past strategies that have focused primarily on addressing the urban/suburban ozone problem to one that considers the problem in a more regional context.

Further analysis of the spatial patterns of 8hr versus 1hr exceedances is in progress. As expected, the Mountain Counties Air Basin shows a significant effect from the proposed 8hr standard.

**Table 2.1-1.
Populations and Areas for Central California Metropolitan Statistical Areas**

State	Metropolitan Area	TYPE	Counties	1990 Population	1995 Est. Population	1995 pop density (km ²)	Area (km ²)
CA	Bakersfield, CA	MSA	Kern County	543,477	617,528	29.3	21086.7
CA	Chico-Paradise, CA	MSA	Butte County	182,120	192,880	45.4	4246.6
CA	Fresno, CA	MSA	Fresno County Madera County	755,580	844,293	40.2	20983.3
CA	Riverside-San Bernardino, CA	PMSA	Riverside County San Bernardino County	2,588,793	2,949,387	41.8	70629.2
CA	Ventura, CA	PMSA	Ventura County	669,016	710,018	148.5	4781.0
CA	Merced, CA	MSA	Merced County	178,403	194,407	38.9	4995.8
CA	Modesto, CA	MSA	Stanislaus County	370,522	410,870	106.1	3870.9
CA	Sacramento, CA	PMSA	El Dorado County Placer County Sacramento County	1,340,010	1,456,955	137.8	10571.3
CA	Yolo, CA	PMSA	Yolo County	141,092	147,769	56.4	2622.2
CA	Salinas, CA	MSA	Monterey County	355,660	348,841	40.5	8603.8
CA	Oakland, CA	PMSA	Alameda County Contra Costa County	2,082,914	2,195,411	581.5	3775.7
CA	Sacramento-Yolo, CA	CMSA	El Dorado County Placer County Sacramento County Yolo County	1,481,220	1,604,724	121.1	13250.4
CA	San Francisco, CA	PMSA	Marin County San Francisco County San Mateo County	1,603,678	1,645,815	625.7	2630.4
CA	San Francisco-Oakland-San Jose, CA	CMSA	Alameda County Contra Costa County Marin County San Francisco County San Mateo County Santa Clara County Santa Cruz County Sonoma County Napa County Solano County	6,249,881	6,539,602	341.1	19173.7
CA	San Jose, CA	PMSA	Santa Clara County	1,497,577	1,565,253	468.0	3344.3
CA	Santa Cruz-Watsonville, CA	PMSA	Santa Cruz County	229,734	236,669	205.0	1154.6
CA	Santa Rosa, CA	PMSA	Sonoma County	388,222	414,569	101.6	4082.4
CA	Vallejo-Fairfield-Napa, CA	PMSA	Napa County Solano County	451,186	481,885	117.6	4097.5
CA	San Luis Obispo-Atascadero-Paso Robles, CA	MSA	San Luis Obispo County	217,162	226,071	26.4	8558.6
CA	Santa Barbara-Santa Maria-Lompoc, CA	MSA	Santa Barbara County	369,608	381,401	53.8	7092.6
CA	Stockton-Lodi, CA	MSA	San Joaquin County	480,628	523,969	144.6	3624.5
CA	Visalia-Tulare-Porterville, CA	MSA	Tulare County	311,921	346,843	27.8	12495.0

**Table 2.2-1a
Linked Master Ozone Monitoring Site List**

LADAM #	AIRS Site	Site		Air Basin	County	Location Type	Data Record		Link #	Elevation		
		Moniker	Short Name				Begin	End		Latitude	Longitude	(msl)
2008	060830008	ECP	El_Capitan_B	South Central Coast	Santa Barbara	Rural	5/1/90	10/31/98		34.4624	-120.0245	30
2013	060190007	FSD	Fresno-Drmond	San Joaquin Valley	Fresno	Suburban	5/1/90	9/30/98		36.7019	-119.7391	162
2016	060530002	CMV	Carm_Val-Frd	North Central Coast	Monterey	Suburban	5/1/90	10/31/98		36.4815	-121.7329	131
2032	061072002	VCS	Visalia-NChu	San Joaquin Valley	Tulare	Urban/Center City	5/1/90	10/31/98		36.3328	-119.2907	92
2070	060851002	MVC	Mtn_View-Cst	San Francisco Bay Area	Santa Clara	Suburban	5/1/90	10/31/98		37.3724	-122.0767	24
2088	061112003	VTE	Emma_Wood_SB	South Central Coast	Ventura	Suburban	5/1/90	10/31/98		34.2804	-119.3153	3
2094	060771002	SOH	Stockton-Haz	San Joaquin Valley	San Joaquin	Urban/Center City	5/1/90	9/30/98		37.9508	-121.2692	13
2102	060133001	PBG	Pittsburg-10th	San Francisco Bay Area	Contra Costa	Urban/Center City	5/1/90	10/31/98		38.0296	-121.8969	2
2105	060970003	SRF	S_Rosa-5th	San Francisco Bay Area	Sonoma	Urban/Center City	5/1/90	10/31/98		38.4436	-122.7092	49
2114	060194001	PLR	Parlier	San Joaquin Valley	Fresno	Rural	5/1/90	9/30/98		36.5967	-119.5042	166
2115	060070002	CHM	Chico-Manznt	Sacramento Valley	Butte	Suburban	5/1/90	10/31/98		39.7569	-121.8595	61
2123	060670002	SNH	N_High-Blckf	Sacramento Valley	Sacramento	Suburban	5/1/90	10/31/98		38.7122	-121.3810	27
2125	060811001	RED	Redwood_City	San Francisco Bay Area	Santa Mateo	Suburban	5/1/90	10/31/98		37.4823	-122.2034	5
2143	061130004	DVS	Davis-UCD	Sacramento Valley	Yolo	Rural	5/1/90	10/31/98		38.5352	-121.7746	16
2161	060831007	SMY	S_Maria-SBrd	South Central Coast	Santa Barbara	Suburban	5/1/90	10/31/98		34.9507	-120.4341	76
2208	060571001	TRU	Truckee-Fire	Mountain Counties	Nevada	Urban/Center City	10/31/92	10/31/98		39.3302	-120.1808	1676
2225	060010005	OKA	Oakland-Alic	San Francisco Bay Area	Alameda	Urban/Center City	5/1/90	10/31/98		37.8014	-122.2672	7
2293	060011001	FCW	Fremont-Chpl	San Francisco Bay Area	Alameda	Suburban	5/1/90	10/31/98		37.5357	-121.9618	18
2312	060290007	EDS	Edison	San Joaquin Valley	Kern	Rural	5/1/90	10/31/98		35.3452	-118.8521	128
2320	060850002	GRY	Gilroy-9th	San Francisco Bay Area	Santa Clara	Suburban	5/1/90	10/31/98		36.9999	-121.5752	55
2321	060793001	MBP	Morro Bay	South Central Coast	San Luis Obispo	Urban/Center City	5/1/90	10/31/98		35.3668	-120.8450	18
2329	060870003	DVP	Davenport	North Central Coast	Santa Cruz	Rural	5/1/90	10/31/98		37.0120	-122.1929	0
2360	060832004	LOM	Lompoc-S_HSt	South Central Coast	Santa Barbara	Urban/Center City	5/16/90	10/31/98		34.6360	-120.4541	24
2372	060010003	LVF	Livmor-Old1	San Francisco Bay Area	Alameda	Urban/Center City	5/1/90	10/31/98		37.6849	-121.7657	146
2373	060750005	SFA	S_F-Arkansas	San Francisco Bay Area	San Francisco	Urban/Center City	5/1/90	10/31/98		37.7661	-122.3978	5
2397	060950002	FFD	Fairfld-AQMD	San Francisco Bay Area	Solano	Urban/Center City	5/1/90	10/31/98		38.2368	-122.0561	3
2410	060950004	VJO	Vallejo-304T	San Francisco Bay Area	Solano	Urban/Center City	5/1/90	10/31/98		38.1029	-122.2369	23
2413	060850004	SJ4	San_Jose-4th	San Francisco Bay Area	Santa Clara	Urban/Center City	5/1/90	10/31/98		37.3400	-121.8875	24
2500	060830010	SBC	S_Barbr-WCr1	South Central Coast	Santa Barbara	Urban/Center City	5/1/90	10/31/98		34.4208	-119.7007	16
2553	060770009	SOM	Stockton-EMr	San Joaquin Valley	San Joaquin	Urban/Center City	5/1/90	9/30/98		37.9056	-121.1461	17
2593	060833001	SYN	S_Ynez-Airpt	South Central Coast	Santa Barbara	Rural	5/1/90	10/31/98		34.6078	-120.0734	204
2613	060851001	LGS	Los Gatos	San Francisco Bay Area	Santa Clara	Urban/Center City	5/1/90	10/31/98		37.2279	-121.9792	183
2622	060410001	SRL	San Rafael	San Francisco Bay Area	Marin	Urban/Center City	5/1/90	10/31/98		37.9728	-122.5184	1
2628	060690002	HST	Hollistr-Frv	North Central Coast	San Benito	Rural	5/1/90	10/31/98		36.8432	-121.3620	126
2655	060550003	NJS	Napa-Jffrsn	San Francisco Bay Area	Napa	Urban/Center City	5/1/90	10/31/98		38.3115	-122.2942	12
2671	060792001	GCL	Grover_City	South Central Coast	San Luis Obispo	Suburban	5/1/90	10/31/98		35.1241	-120.6322	4
2702	061110004	PIR	Piru-2mi_SW	South Central Coast	Ventura	Rural	5/1/90	10/31/98		34.4025	-118.8244	182
2709	060792002	SLM	S_L_O-Marsh	South Central Coast	San Luis Obispo	Urban/Center City	5/1/90	10/31/98		35.2826	-120.6546	66
2731	060670006	SDP	Sacto-DelPas	Sacramento Valley	Sacramento	Suburban	5/1/90	10/31/98		38.6141	-121.3669	25
2744	060111002	CSS	Colusa-Sunrs	Sacramento Valley	Colusa	Rural	7/18/96	10/31/98	6	39.1886	-121.9989	17
2752	060932001	YRE	Yreka-Fthill	Northeast Plateau	Siskiyou	Suburban	5/1/90	9/30/98		41.7293	-122.6354	800
2756	061110005	VTA	WCasitasPass	South Central Coast	Ventura	Rural	5/1/90	10/31/98		34.3842	-119.4145	319
2772	060290232	OLD	Oildale-3311	San Joaquin Valley	Kern	Suburban	5/1/90	10/31/98		35.4385	-119.0168	180

Table 2.2-1a (continued)
Linked Master Ozone Monitoring Stie List

LADAM #	AIRS Site	Site		Air Basin	County	Location Type	Data Record		Link #	Latitude	Longitude	Elevation (msl)
		Moniker	Short Name				Begin	End				
2789	060531002	SL2	Salinas-Ntvd	North Central Coast	Monterey	Suburban	5/1/90	10/31/98		36.6986	-121.6354	13
2804	060131002	BTI	Bethel_Is_Rd	San Francisco Bay Area	Contra Costa	Rural	5/1/90	10/31/98		38.0067	-121.6414	0
2806	060012001	HLM	Hayward	San Francisco Bay Area	Alameda	Rural	5/1/90	10/31/98		37.6542	-122.0305	287
2829	060890004	RDH	Redding-HDrf	Sacramento Valley	Shasta	Suburban	5/1/90	10/31/98		40.5503	-122.3802	143
2831	060130002	CCD	Concord-2975	San Francisco Bay Area	Contra Costa	Suburban	5/1/90	10/31/98		37.9391	-122.0247	26
2833	060990005	M14	Modesto-14th	San Joaquin Valley	Stanislaus	Urban/Center City	5/1/90	10/31/98		37.6424	-120.9936	27
2844	060190242	FSS	Fresno-Sky#2	San Joaquin Valley	Fresno	Suburban	7/29/91	9/30/98		36.8411	-119.8764	98
2848	061010002	PGV	Plsnt_Grv4mi	Sacramento Valley	Sutter	Rural	5/1/90	9/30/98		38.7658	-121.5191	50
2880	061112002	SIM	Simi_V-CchrS	South Central Coast	Ventura	Suburban	5/1/90	10/31/98		34.2775	-118.6847	310
2891	060610002	AUB	Auburn-DwttC	Sacramento Valley	Placer	Suburban	5/1/90	10/10/97		38.9395	-121.1054	433
2894	060530005	KCM	King_Cty-Mtz	North Central Coast	Monterey	Rural	6/30/90	9/30/98		36.2269	-121.1153	116
2914	060333001	LKL	Lakepor-Lake	Lake County	Lake	Suburban	5/1/90	10/31/98		39.0330	-122.9219	405
2919	060290008	MCS	Maricopa-Stn	San Joaquin Valley	Kern	Suburban	5/1/90	9/30/98		35.0519	-119.4037	289
2923	060710001	BSW	Barstow	Mojave Desert	San Bernardino	Urban/Center City	5/1/90	10/31/98		34.8950	-117.0236	692
2939	060530006	MON	Montery-SlvC	North Central Coast	Monterey	Rural	5/1/92	10/31/98		36.5722	-121.8117	73
2941	060295001	ARV	Arvin-Br_Mtn	San Joaquin Valley	Kern	Rural	5/1/90	10/31/98		35.2087	-118.7763	145
2954	060831018	GVB	Gaviota-GT#B	South Central Coast	Santa Barbara	Rural	5/1/90	10/31/98		34.5275	-120.1964	305
2955	060790005	PRF	Pas_Rob-Snta	South Central Coast	San Luis Obispo	Suburban	8/31/91	10/31/98	21	35.6316	-120.6900	100
2956	060610006	ROS	Rosevil-NSun	Sacramento Valley	Placer	Suburban	5/1/93	9/30/98	9	38.7500	-121.2640	161
2957	060831014	LPD	Los_PadresNF	South Central Coast	Santa Barbara	Rural	5/2/90	10/31/98		34.5416	-119.7913	547
2958	061010003	YAS	Yuba_Cty-Alm	Sacramento Valley	Sutter	Suburban	5/1/90	10/31/98		39.1388	-121.6191	20
2965	060798001	ATL	Atascadero	South Central Coast	San Luis Obispo	Suburban	5/1/90	10/31/98		35.4919	-120.6681	262
2968	061090005	SNB	Sonora-Brret	Mountain Counties	Tuolumne	Urban/Center City	7/31/92	7/31/98		37.9816	-120.3786	571
2969	060852005	SJD	San_Jose-935	San Francisco Bay Area	Santa Clara	Rural	8/24/92	10/31/98		37.3913	-121.8420	63
2972	060893003	LNP	Lasn_Vlcn_NP	Sacramento Valley	Shasta	Rural	5/1/90	10/31/98		40.5397	-121.5816	1788
2973	060010006	SEH	Sn_Lndro-Hos	San Francisco Bay Area	Alameda	Suburban	8/2/90	10/31/98		37.7098	-122.1164	36
2977	060670011	ELK	Elk_Grv-Brev	Sacramento Valley	Sacramento	Rural	5/1/93	10/31/98		38.3028	-121.4207	6
2979	060792004	NGR	Nipomo-Gudlp	South Central Coast	San Luis Obispo	Rural	6/6/91	10/31/98	20	35.0202	-120.5614	60
2981	060296001	SHA	Shafter-Wlkr	San Joaquin Valley	Kern	Suburban	5/1/90	10/31/98		35.5033	-119.2721	126
2983	060690003	PIN	Pinn_Nat_Mon	North Central Coast	San Benito	Rural	5/1/90	10/31/98		36.4850	-120.8444	335
2984	061110007	THM	1000_Oaks-Mr	South Central Coast	Ventura	Suburban	5/1/92	10/31/98	23	34.2198	-118.8671	232
2985	060870004	WAA	Watsonvll-AP	North Central Coast	Santa Cruz	Suburban	7/31/92	10/31/98		36.9337	-121.7816	67
2991	061113001	ELM	El_Rio-Sch#2	South Central Coast	Ventura	Rural	5/1/92	10/31/98	24	34.2520	-119.1545	34
2992	060831013	LHS	Lompoc-HS&P1	South Central Coast	Santa Barbara	Rural	5/1/90	10/31/98		34.7251	-120.4284	244
2993	060050002	JAC	Jackson-CIRd	Mountain Counties	Amador	Suburban	5/14/92	5/31/98		38.3421	-120.7641	377
2996	060990006	TSM	Turlock-SMIn	San Joaquin Valley	Stanislaus	Suburban	5/1/92	9/30/98	18	37.4883	-120.8355	56
3002	060610004	CXC	Colfax-CtyHl	Mountain Counties	Placer	Rural	5/1/92	10/31/97		39.0998	-120.9542	768
3003	060831021	CRP	Carpint-Gbrn	South Central Coast	Santa Barbara	Rural	5/1/90	10/31/98		34.4030	-119.4580	152
3008	060613001	ROC	Rocklin	Sacramento Valley	Placer	Rural	5/1/91	9/30/98	8	38.7890	-121.2070	100
3009	060190008	FSF	Fresno-1st	San Joaquin Valley	Fresno	Suburban	5/1/90	10/31/98		36.7816	-119.7732	96
3010	060450008	UKG	Ukiah-EGobbi	North Coast	Mendocino	Suburban	9/30/92	10/31/98		39.1447	-123.2065	194
3011	060670010	S13	Sacto-T_Strt	Sacramento Valley	Sacramento	Urban/Center City	5/1/90	10/31/98		38.5679	-121.4931	7
3017	060170010	PGN	Plervll-Gold	Mountain Counties	El Dorado	Suburban	5/1/92	10/31/98		38.7247	-120.8220	585

Table 2.2-1a (continued)
Linked Master Ozone Monitoring Site List

LADAM #	AIRS Site	Site		Air Basin	County	Location Type	Data Record		Link #	Latitude	Longitude	Elevation (msl)
		Moniker	Short Name				Begin	End				
3018	060430003	YOT	Yos_NP-Trtle	Mountain Counties	Mariposa	Rural	8/31/90	10/31/98		37.7135	-119.7055	1605
3020	060631006	QUC	Quincy-NChrc	Mountain Counties	Plumas	Urban/Center City	10/31/92	10/31/98		39.9381	-120.9413	1067
3022	060470003	MRA	Merced-SCofe	San Joaquin Valley	Merced	Rural	10/9/91	9/30/98		37.2819	-120.4334	86
3023	060834003	VBS	Van_AFB-STSP	South Central Coast	Santa Barbara	Rural	5/1/90	10/31/98		34.5961	-120.6327	100
3026	060195001	CLO	Clovis	San Joaquin Valley	Fresno	Urban/Center City	9/5/90	9/30/98		36.8194	-119.7165	86
3029	060831020	SBU	S_Barbr-UCSB	South Central Coast	Santa Barbara	Rural	5/1/90	7/15/98		34.4147	-119.8788	9
3032	060890007	ADN	Anderson-Nth	Sacramento Valley	Shasta	Suburban	5/31/93	10/31/98		40.4653	-122.2973	498
3033	060971003	HDM	Healdsb-Aprt	North Coast	Sonoma	Rural	5/1/92	10/31/98		38.6536	-122.9006	30
3036	061070006	SEK	Seq_NP-Kawea	San Joaquin Valley	Tulare	Rural	7/31/96	10/31/98	19	36.5640	-118.7730	1901
3101	060831025	CA1	Capitan-LF#1	South Central Coast	Santa Barbara	Rural	5/1/90	10/31/98		34.4897	-120.0458	0
3116	060450009	WLM	Willits-Main	North Coast	Mendocino	Suburban	6/30/93	10/31/98		39.4030	-123.3491	1377
3117	061010004	SUT	Sutter_Butte	Sacramento Valley	Sutter	Rural	6/30/93	10/31/98		39.1583	-121.7500	640
3121	060290011	MOP	Mojave-Poole	Mojave Desert	Kern	Rural	8/1/93	10/31/98		35.0500	-118.1479	853
3126	060570005	GVL	Grs_Vly-Litn	Mountain Counties	Nevada	Suburban	9/30/93	10/31/98	3	39.2334	-121.0555	853
3129	060311004	HIR	Hanford-Irwn	San Joaquin Valley	Kings	Suburban	5/1/94	9/30/98	15	36.3149	-119.6431	99
3133	060870006	SVD	Scotts_V-Drv	North Central Coast	Santa Cruz	Rural	6/30/94	10/31/98	5	37.0514	-122.0148	122
3137	060210002	WLW	Willows-ELau	Sacramento Valley	Glenn	Suburban	6/16/94	10/31/98	7	39.5170	-122.1895	41
3140	060852006	SMM	San_Martin	San Francisco Bay Area	Santa Clara	Rural	5/1/94	10/31/98		37.0793	-121.6001	87
3144	060090001	SGS	San_Andreas	Mountain Counties	Calaveras	Rural	5/1/94	5/31/98		38.2000	-120.6670	
3145	060290010	BGS	Baker-GS_Hwy	San Joaquin Valley	Kern	Urban/Center City	7/6/94	9/30/98		35.3855	-119.0147	123
3146	060290014	BKA	Baker-5558Ca	San Joaquin Valley	Kern	Urban/Center City	5/1/94	10/31/98	14	35.3561	-119.0402	120
3152	060719002	JSN	Josh_Tr-Mnmt	Mojave Desert	San Bernardino	Rural	9/30/93	10/31/98	1	34.0713	-116.3905	1244
3153	060832011	GNF	Goleta-NFrvw	South Central Coast	Santa Barbara	Suburban	5/1/94	10/31/98	22	34.4455	-119.8287	50
3155	060953002	VEL	Vacavil-Alli	Sacramento Valley	Solano	Suburban	5/1/95	10/31/98		38.3519	-121.9631	55
3157	060570007	WCM	White_Cld_Mt	Mountain Counties	Nevada	Rural	6/2/95	9/30/98		39.3166	-120.8444	1302
3158	061030004	TSB	Tuscan Butte	Sacramento Valley	Tehama	Rural	6/1/95	9/30/98		40.2617	-122.0911	568
3159	060773003	TPP	Tracy-Patt#2	San Joaquin Valley	San Joaquin	Rural	6/14/95	9/30/98	17	37.7363	-121.5335	31
3160	060190010	FNP	ShavLk-PerRd	San Joaquin Valley	Fresno	Rural	8/31/95	10/31/98		37.1383	-119.2666	0
3161	060430006	JSD	Jerseydale	Mountain Counties	Mariposa	Rural	7/18/95	10/31/98		37.5500	-119.8436	0
3164	061090006	FML	Sonora-OakRd	Mountain Counties	Tuolumne	Rural	8/31/95	7/31/98		38.0505	-120.2997	0
3172	061111004	OJO	Ojai-OjaiAve	South Central Coast	Ventura	Suburban	5/1/96	10/31/98	25	34.4166	-119.2458	262
3177	060832012	SRI	SRosaIsland	South Central Coast	Santa Barbara	Rural	5/1/96	10/31/98		34.0166	-120.0500	0
3187	060670012	FLN	Folsom-Ntma	Sacramento Valley	Sacramento	Suburban	8/31/96	10/31/98	10	38.6838	-121.1627	98
3196	060170020	CUS	Cool-Hwy193	Mountain Counties	El Dorado	Rural	5/31/96	9/30/98		38.8905	-121.0000	0
3197	061030005	RBO	Red_Blif-Oak	Sacramento Valley	Tehama	Urban/Center City	7/31/96	9/30/98	11	40.1763	-122.2374	98
3200	060870007	SCQ	S_Cruz-Soqul	North Central Coast	Santa Cruz	Suburban	9/24/96	10/31/98	4	36.9858	-121.9930	78
3207	060131003	SPE	San Pablo	San Francisco Bay Area	Contra Costa	Urban/Center City	5/9/97	10/31/98	13	37.9500	-122.3561	15
3211	060390004	M29	Madera	San Joaquin Valley	Madera	Rural	8/21/97	9/30/98	16	36.8669	-120.0100	
3215	060711234	TRT	Trona-Telegraph	Mojave Desert	San Bernardino	Rural	5/1/97	10/31/98	2	35.7639	-117.3961	
3249	061131003	WLG	Woodland-GibsonRd	Sacramento Valley	Yolo	Suburban	5/31/98	10/31/98	12	38.6619	-121.7278	

Table 2.2-1b
Ozone Monitoring Sites Linked in Time for Longer Period of Record

L#	Retained Site	StartDate1	Linked Site #1 Preceding Retained Sited				Linked Site #2 Preceding Linked Site #1			
			LSite 1	StartDate1	StopDate1	Dist1_km	LSite 2	StartDate2	StopDate2	Dist2_km
1	Josh_Tr-Mmnt	9/30/93	Josh_Tr-LHrs	5/1/90	9/22/93	19.5				
2	Trona-Telegraph	5/1/97	Trona-Market	5/1/90	10/31/93	1.8	Trona-Athol	5/1/93	10/31/96	2.7
3	Grs_Vly-Litn	9/30/93	Nvda_Cty-Wll	5/31/90	9/30/92	5.6				
4	S_Cruz-Soqul	9/24/96	S_Cruz-Bstwc	5/1/90	9/12/96	0.5				
5	Scotts_V-Drv	6/30/94	Scotts_V-Vin	8/12/92	10/31/94	2.3				
6	Colusa-Sunrs	7/18/96	Colusa-FairG	10/3/91	10/15/96	2.2				
7	Willows-ELau	6/16/94	Willows-NVil	7/24/90	6/2/94	1.7				
8	Rocklin	5/1/91	Rocklin-Sier	5/1/90	10/31/90	0.3				
9	Rosevil-NSun	5/1/93	Citrus_Hghts	5/1/90	10/31/92	5.7				
10	Folsom-Ntma	8/31/96	Folsom-CityC	5/1/90	10/31/96	2.2				
11	Red_BlF-Oak	7/31/96	Red_BlF-Wlnt	7/6/90	10/31/95	1.6				
12	Woodland-GibsonRd	5/31/98	Woodlnd-Main	5/1/90	8/30/91	5.4	Woodlnd-Sutr	5/1/92	10/31/97	7.7
13	San Pablo	5/9/97	Richmnd-13th	5/1/90	5/6/97	0.1				
14	Baker-5558Ca	5/1/94	Baker-Chestr	5/1/90	10/31/93	1.9				
15	Hanford-Irwn	5/1/94	Hanford	5/1/90	7/30/93	2.3				
16	Madera	8/21/97	Madera-HD#2	5/1/90	9/30/96	10.1				
17	Tracy-Patt#2	6/14/95	Tracy-Patrs	8/18/94	6/13/95	0.4				
18	Turlock-SMin	5/1/92	Turlock-MV#1	5/1/90	8/31/92	4.7				
19	Seq_NP-Kawea	7/31/96	Seq_NP-Giant	5/1/90	7/31/96	0.6				
20	Nipomo-Gudlp	6/6/91	Nipomo-Eclps	6/12/90	5/23/91	2.5				
21	Pas_Rob-Snta	8/31/91	Pas_Rob-10th	5/1/90	9/17/90	0.2				
22	Goleta-NFrvw	5/1/94	Goleta	5/1/90	10/31/93	0.0				
23	1000_Oaks-Mr	5/1/92	1000_Oaks-Wn	5/1/90	10/31/91	2.9				
24	El_Rio-Sch#2	5/1/92	El Rio	5/1/90	10/31/91	1.1				
25	Ojai-OjaiAve	5/1/96	Ojai-1768Mar	5/1/90	10/31/95	3.5				

Table 2.2-2
Summary of Trends in Daily 1hr and 8hr Ozone Maxima During May-October, 1990-98

Basin	Standard	Variable	Year									Group Annual Means ^a		
			1990	1991	1992	1993	1994	1995	1996	1997	1998	1990-95	1996-98	1990-98
North Coast	1hr	Max Daily Max			0.09	0.09	0.1	0.1	0.08	0.1	0.13	0.095	0.103	0.099
		Avg Daily Max			0.045	0.040	0.043	0.041	0.039	0.039	0.042	0.042	0.040	0.041
		Count	0	0	215	487	540	543	264	545	548	1785	1357	3142
	8hr	Max Daily Max			0.072	0.073	0.08	0.09	0.071	0.091	0.106	0.079	0.089	0.083
		Avg Daily Max			0.038	0.033	0.035	0.034	0.037	0.033	0.035	0.035	0.035	0.035
		Count	0	0	216	490	545	542	240	544	541	1793	1325	3118
Northeast Plateau	1hr	Max Daily Max	0.07	0.05	0.08	0.07	0.08	0.07	0.07	0.082	0.078	0.074	0.077	0.075
		Avg Daily Max	0.042	0.033	0.048	0.041	0.050	0.044	0.047	0.050	0.053	0.045	0.050	0.047
		Count	107	21	113	175	181	184	105	182	146	781	433	1214
	8hr	Max Daily Max	0.068	0.046	0.073	0.07	0.068	0.062	0.063	0.074	0.071	0.068	0.069	0.069
		Avg Daily Max	0.036	0.025	0.043	0.036	0.044	0.038	0.040	0.044	0.046	0.039	0.044	0.041
		Count	108	23	113	174	181	184	106	182	146	783	434	1217
Lake County	1hr	Max Daily Max	0.09	0.08	0.07	0.08	0.09	0.07	0.09	0.08	0.08	0.082	0.083	0.083
		Avg Daily Max	0.040	0.047	0.043	0.039	0.053	0.037	0.041	0.039	0.039	0.043	0.040	0.042
		Count	184	183	91	184	184	184	184	184	184	1010	552	1562
	8hr	Max Daily Max	0.063	0.066	0.057	0.072	0.075	0.063	0.07	0.065	0.076	0.068	0.070	0.069
		Avg Daily Max	0.034	0.041	0.037	0.033	0.046	0.031	0.035	0.033	0.034	0.037	0.034	0.036
		Count	184	183	92	184	184	184	184	184	184	1011	552	1563
Mountain Counties	1hr	Max Daily Max	0.15	0.11	0.13	0.12	0.13	0.146	0.138	0.145	0.163	0.131	0.149	0.137
		Avg Daily Max	0.066	0.074	0.071	0.064	0.068	0.067	0.069	0.064	0.062	0.067	0.065	0.066
		Count	212	293	849	1217	1568	1670	2322	2178	1549	5809	6049	11858
	8hr	Max Daily Max	0.115	0.102	0.112	0.111	0.108	0.113	0.113	0.112	0.127	0.110	0.117	0.113
		Avg Daily Max	0.059	0.066	0.063	0.056	0.061	0.060	0.062	0.057	0.056	0.060	0.058	0.059
		Count	214	294	852	1218	1572	1674	2324	2181	1554	5824	6059	11883
Sacramento Valley	1hr	Max Daily Max	0.15	0.19	0.17	0.15	0.145	0.156	0.157	0.125	0.16	0.160	0.147	0.156
		Avg Daily Max	0.061	0.065	0.067	0.059	0.066	0.062	0.065	0.058	0.063	0.063	0.062	0.062
		Count	2713	2546	2880	3460	3426	3938	3876	3993	3550	18963	11419	30382
	8hr	Max Daily Max	0.127	0.14	0.122	0.12	0.121	0.128	0.126	0.107	0.137	0.126	0.123	0.125
		Avg Daily Max	0.051	0.054	0.056	0.050	0.056	0.052	0.055	0.049	0.054	0.053	0.053	0.053
		Count	2713	2547	2880	3463	3428	3940	3885	3993	3556	18971	11434	30405

^a Includes only years with >75% data recovery

Table 2.2-2 (continued)
Summary of Trends in Daily 1hr and 8hr Ozone Maxima During May-October, 1990-98

Basin	Standard	Variable	Year									Group Annual Means ^a		
			1990	1991	1992	1993	1994	1995	1996	1997	1998	1990-95	1996-98	1990-98
San Francisco Bay Area	1hr	Max Daily Max	0.13	0.14	0.13	0.13	0.13	0.155	0.138	0.114	0.147	0.136	0.133	0.135
		Avg Daily Max	0.041	0.042	0.043	0.044	0.042	0.047	0.046	0.040	0.044	0.043	0.043	0.043
		Count	3561	3657	3722	3854	4043	4037	3923	4039	3961	22874	11923	34797
	8hr	Max Daily Max	0.105	0.108	0.101	0.112	0.097	0.115	0.112	0.084	0.111	0.106	0.102	0.105
		Avg Daily Max	0.033	0.034	0.035	0.035	0.034	0.037	0.037	0.033	0.035	0.035	0.035	0.035
		Count	3562	3658	3722	3851	4043	4034	3924	4039	3961	22870	11924	34794
North Central Coast	1hr	Max Daily Max	0.12	0.14	0.11	0.11	0.101	0.138	0.12	0.112	0.124	0.120	0.119	0.119
		Avg Daily Max	0.046	0.048	0.045	0.046	0.043	0.045	0.047	0.043	0.045	0.045	0.045	0.045
		Count	1187	1273	1560	1795	1814	1825	1802	1825	1795	9454	5422	14876
	8hr	Max Daily Max	0.095	0.108	0.09	0.087	0.092	0.102	0.101	0.091	0.097	0.096	0.096	0.096
		Avg Daily Max	0.039	0.042	0.039	0.040	0.037	0.039	0.040	0.037	0.039	0.039	0.039	0.039
		Count	1186	1272	1565	1790	1810	1825	1800	1825	1794	9448	5419	14867
San Joaquin Valley	1hr	Max Daily Max	0.17	0.18	0.16	0.16	0.175	0.173	0.165	0.147	0.169	0.170	0.160	0.167
		Avg Daily Max	0.074	0.078	0.076	0.076	0.075	0.075	0.079	0.071	0.076	0.075	0.075	0.075
		Count	3074	3378	3390	3508	3828	4051	4165	4083	3549	21229	11797	33026
	8hr	Max Daily Max	0.123	0.13	0.121	0.125	0.129	0.134	0.137	0.127	0.136	0.127	0.133	0.129
		Avg Daily Max	0.063	0.066	0.064	0.065	0.064	0.064	0.068	0.061	0.066	0.064	0.065	0.064
		Count	3066	3370	3391	3508	3827	4052	4167	4084	3552	21214	11803	33017
South Central Coast	1hr	Max Daily Max	0.17	0.17	0.15	0.146	0.164	0.169	0.158	0.137	0.174	0.162	0.156	0.160
		Avg Daily Max	0.055	0.056	0.054	0.053	0.056	0.056	0.057	0.053	0.053	0.055	0.054	0.055
		Count	4592	4525	4699	4769	4565	4681	4918	4923	4831	27831	14672	42503
	8hr	Max Daily Max	0.143	0.14	0.125	0.129	0.132	0.144	0.127	0.114	0.151	0.144	0.151	0.151
		Avg Daily Max	0.047	0.049	0.047	0.046	0.048	0.048	0.050	0.047	0.046	0.076	0.048	0.065
		Count	4584	4520	4697	4766	4559	4678	4913	4915	4828	27804	14656	42460
Mojave Desert	1hr	Max Daily Max	0.13	0.13	0.12	0.14	0.165	0.151	0.146	0.149	0.142	0.139	0.146	0.141
		Avg Daily Max	0.072	0.072	0.069	0.072	0.079	0.072	0.077	0.072	0.072	0.073	0.074	0.073
		Count	436	475	338	561	723	714	726	711	692	3247	2129	5376
	8hr	Max Daily Max	0.102	0.115	0.097	0.114	0.127	0.106	0.117	0.122	0.123	0.110	0.121	0.114
		Avg Daily Max	0.062	0.063	0.059	0.063	0.069	0.063	0.068	0.064	0.064	0.063	0.065	0.064
		Count	435	475	339	562	727	713	726	711	685	3251	2122	5373

^a Includes only years with >75% data recovery

Table 2.2.3
Annual Maximum of Daily Maximum Ozone Concentrations in Central California During May to October, 1990-98

(This section 2 table or figure is a separate handout for this draft)

Table 2.2.3
Annual Maximum of Daily Maximum Ozone Concentrations in Central California During May to October, 1990-98^a

(This section 2 table or figure is a separate handout for this draft)

**Table 2.2.3 (cont.)
Annual Maximum of Daily Maximum Ozone Concentrations in Central California During May to October,
1990-98^a**

(This section 2 table or figure is a separate handout for this draft)

Table 2.2.3 (cont.)
Annual Maximum of Daily Maximum Ozone Concentrations in Central California During May to October,
1990-98^a

(This section 2 table or figure is a separate handout for this draft)

Figure 2.2.4
Annual Exceedances of the 1-hr and 8-hr Ozone Standards in Central California During May to October, 1990-98 ^a

(This section 2 table or figure is a separate handout for this draft)

Figure 2.2.4 (cont.)

Annual Exceedances of the 1-hr and 8-hr Ozone Standards in Central California During May to October, 1990-98 ^a

(This section 2 table or figure is a separate handout for this draft)

Figure 2.2.4 (cont.)

Annual Exceedances of the 1-hr and 8-hr Ozone Standards in Central California During May to October, 1990-98 ^a

(This section 2 table or figure is a separate handout for this draft)

Figure 2.2.4 (cont.)

Table 2.2.2 Annual Exceedances of the 1-hr and 8-hr Ozone Standards in Central California During May to October, 1990-98

(This section 2 table or figure is a separate handout for this draft)

Table 2.2.5
Average Annual Exceedances of the 1-hr and 8-hr Ozone Standards in Central California by Month During May to October, 1990-98

(This section 2 table or figure is a separate handout for this draft)

Table 2.2.5 (cont.)

Average Annual Exceedances of the 1-hr and 8-hr Ozone Standards in Central California by Month During May to October, 1990-98

(This section 2 table or figure is a separate handout for this draft)

Table 2.2.5 (cont.)

Average Annual Exceedances of the 1-hr and 8-hr Ozone Standards in Central California by Month During May to October, 1990-98

(This section 2 table or figure is a separate handout for this draft)

Table 2.2.5 (cont.)

Average Annual Exceedances of the 1-hr and 8-hr Ozone Standards in Central California by Month During May to October, 1990-98

(This section 2 table or figure is a separate handout for this draft)

Table 2.2.6b cont. Percentage of Daily Ozone 8-hr Maxima by Start-Hour in Central California During May to October, 1990-98

(This section 2 table or figure is a separate handout for this draft)

(This section 2 table or figure is a separate handout for this draft)

Table 2.3-1
1996 Daily Average ROG Emissions by Air Basins in the CCOS Domain

SOURCE CATEGORIES	Mountain Counties	Bay Area	Sacramento Valley	San Joaquin Valley	North Central Coast	South Central Coast
STATIONARY						
FUEL COMBUSTION						
electric utilities	0.1	0.1	0.1	0.0	0.1	0.1
cogeneration	0.4	0.2	0.1	1.0	0.4	0.0
oil and gas production (combustion)	0.0	0.0	0.3	5.3	0.0	0.5
petroleum refining (combustion)	0.0	0.5	0.0	0.0	0.0	0.0
manufacturing and industrial	0.4	0.7	0.3	0.2	0.0	0.1
food and agricultural processing	0.0	0.0	0.0	2.4	0.0	0.2
service and commercial	0.0	0.7	0.3	2.2	0.0	0.2
other (fuel combustion)	0.0	0.5	0.2	0.1	0.0	0.0
WASTE DISPOSAL						
sewage treatment	0.0	0.2	0.0	0.0	0.0	0.0
landfills	0.0	5.0	0.8	5.0	2.3	1.0
incinerators	0.0	0.0	0.0	0.0	0.0	0.0
soil remediation	0.0	0.0	0.0	0.0	0.0	0.0
other (waste disposal)	0.0	0.0	0.0	1.3	0.0	0.0
CLEANING AND SURFACE COATINGS						
laundry	0.4	3.8	1.7	0.6	0.9	0.3
degreasing	1.0	5.8	5.0	7.0	1.8	3.5
coatings and related process solvents	2.5	26.3	16.6	16.1	5.8	6.1
printing	0.0	6.0	1.3	1.3	0.2	1.0
other (cleaning and surface coatings)	0.4	11.3	2.6	4.0	0.6	2.2
PETROLEUM PRODUCTION AND MARKETING						
oil and gas production	0.0	0.2	10.0	51.8	0.9	6.8
petroleum refining	0.0	19.2	0.0	1.3	0.0	0.5
petroleum marketing	0.8	22.6	5.6	6.6	1.3	2.4
other (petroleum production and marketing)	0.0	5.5	0.0	0.3	0.0	0.0
INDUSTRIAL PROCESSES						
chemical	0.0	2.1	3.2	1.5	0.1	0.1
food and agriculture	0.0	1.7	0.8	9.0	0.3	0.2
mineral processes	0.0	0.6	1.0	0.2	0.0	0.0
metal processes	0.0	0.1	0.0	0.1	0.0	0.0
wood and paper	0.5	0.0	0.9	0.0	0.0	0.1
glass and related products	0.0	0.0	0.0	0.1	0.0	0.0
electronics	0.0	0.0	0.0	0.0	0.1	0.0
other (industrial processes)	0.5	7.1	0.4	0.0	0.0	0.1
AREA-WIDE						
SOLVENT EVAPORATION						
consumer products	3.0	47.0	16.0	21.0	4.5	10.1
architectural coatings and related solvents	2.2	23.7	10.0	10.6	2.6	5.1
pesticides/fertilizers	0.5	4.9	7.5	46.3	10.9	6.5
asphalt paving	3.8	0.2	7.5	1.1	2.2	0.8
refrigerants	0.0	0.0	0.0	0.0	0.0	0.0
other (solvent evaporation)	0.0	0.0	0.0	0.9	0.0	0.2
MISCELLANEOUS PROCESSES						
residential fuel combustion	7.3	8.8	8.2	5.6	1.7	2.0
farming operations	0.0	3.8	2.1	70.1	0.0	0.0
construction and demolition	0.0	0.0	0.0	0.0	0.0	0.0
paved road dust	0.0	0.0	0.0	0.0	0.0	0.0
unpaved road dust	0.0	0.0	0.0	0.0	0.0	0.0
fugitive windblown dust	0.0	0.0	0.0	0.0	0.0	0.0
fires	0.0	0.2	0.1	0.2	0.0	0.0
waste burning and disposal	4.8	0.7	15.8	17.0	1.3	3.5
utility equipment	6.3	8.5	4.7	4.9	1.3	1.9
other (miscellaneous processes)	0.0	0.9	1.0	0.4	0.1	0.4

Table 2.3-1 (continued)
1996 Daily Average ROG Emissions by Air Basins in the CCOS Domain

SOURCE CATEGORIES	Mountain Counties	Bay Area	Sacramento Valley	San Joaquin Valley	North Central Coast	South Central Coast
MOBILE						
ON-ROAD MOTOR VEHICLES						
light duty passenger	13.5	158.3	68.5	82.9	15.5	32.5
light and medium duty trucks	0.0	0.0	0.0	0.0	0.0	0.0
light duty trucks	9.4	66.7	38.2	54.3	8.0	16.1
medium duty trucks	1.2	8.5	4.8	6.7	1.0	2.1
heavy duty gas trucks (all)	0.0	0.0	0.0	0.0	0.0	0.0
light heavy duty gas trucks	0.3	2.1	1.5	2.7	0.3	0.5
medium heavy duty gas trucks	0.2	1.0	0.7	1.2	0.2	0.3
heavy duty diesel trucks (all)	0.0	0.0	0.0	0.0	0.0	0.0
light heavy duty diesel trucks	0.1	0.6	0.5	0.7	0.1	0.2
medium heavy duty diesel trucks	0.2	1.4	1.2	1.6	0.3	0.4
heavy heavy duty diesel trucks	0.5	3.9	3.4	4.5	0.8	1.1
motorcycles	0.2	1.8	0.7	1.2	0.2	0.5
heavy duty diesel urban buses	0.0	0.5	0.1	0.1	0.0	0.0
other (on-road motor vehicles)	0.0	0.0	0.0	0.0	0.0	0.0
OTHER MOBILE SOURCES						
aircraft	0.1	10.3	2.4	10.0	0.3	1.1
trains	0.2	0.5	0.7	0.9	0.1	0.2
ships and commercial boats	0.0	0.7	0.1	0.1	0.0	0.8
recreational boats	10.0	11.3	10.7	7.7	2.3	3.2
off-road recreational vehicles	17.8	2.3	5.2	5.7	0.6	1.2
commercial/industrial mobile equipment	0.6	15.4	2.3	4.7	0.9	1.6
farm equipment	0.6	0.8	2.6	5.2	1.0	1.5
other (other mobile sources)	0.0	0.0	0.0	0.0	0.0	0.0
NATURAL (NON-ANTHROPOGENIC)						
geogenic sources	0.0	0.0	0.1	0.3	0.0	20.8
wildfires	2.3	0.2	3.0	3.5	1.3	4.9
windblown dust	0.0	0.0	0.0	0.0	0.0	0.0
other (natural sources)	0.0	0.0	0.0	0.0	0.0	0.0
TOTALS						
Stationary	7.0	120.2	51.2	117.4	14.8	25.4
Area-Wide	27.9	98.7	72.9	178.1	24.6	30.5
On-Road Motor Vehicles	25.6	244.8	119.6	155.9	26.4	53.7
Other Mobile Sources	29.3	41.3	24.0	34.3	5.2	9.6
Natural	2.3	0.2	3.1	3.8	1.3	25.7
TOTAL	92.1	505.2	270.8	489.5	72.3	144.9

Table 2.3-2
1996 Daily Average NOx Emissions by Air Basins in the CCOS Domain

SOURCE CATEGORIES	Mountain Counties	Bay Area	Sacramento Valley	San Joaquin Valley	North Central Coast	South Central Coast
STATIONARY						
FUEL COMBUSTION						
electric utilities	0.8	11.8	2.0	2.0	7.1	2.4
cogeneration	2.0	9.5	2.3	17.9	0.5	0.7
oil and gas production (combustion)	0.0	0.3	3.6	49.8	0.4	4.0
petroleum refining (combustion)	0.0	32.5	0.0	2.5	0.0	0.3
manufacturing and industrial	2.3	25.5	5.4	26.9	8.1	1.9
food and agricultural processing	0.0	0.6	1.6	37.3	0.1	1.6
service and commercial	0.5	9.5	7.1	25.6	1.2	3.6
other (fuel combustion)	0.2	1.9	1.0	0.9	0.1	0.0
WASTE DISPOSAL						
sewage treatment	0.0	0.1	0.0	0.0	0.0	0.0
landfills	0.0	0.0	0.0	0.0	0.0	0.0
incinerators	0.0	0.2	0.1	0.0	0.0	0.0
soil remediation	0.0	0.0	0.0	0.0	0.0	0.0
other (waste disposal)	0.0	0.0	0.0	0.0	0.0	0.0
CLEANING AND SURFACE COATINGS						
laundry	0.0	0.0	0.0	0.0	0.0	0.0
degreasing	0.0	0.0	0.0	0.0	0.0	0.0
coatings and related process solvents	0.0	0.0	0.0	0.0	0.0	0.0
printing	0.0	0.0	0.0	0.0	0.0	0.0
other (cleaning and surface coatings)	0.0	0.0	0.0	0.0	0.0	0.0
PETROLEUM PRODUCTION AND MARKETING						
oil and gas production	0.0	0.0	2.4	0.2	0.0	0.1
petroleum refining	0.0	8.2	0.0	0.1	0.0	0.1
petroleum marketing	0.0	0.0	0.0	0.0	0.0	0.1
other (petroleum production and marketing)	0.0	0.0	0.0	0.0	0.0	0.0
INDUSTRIAL PROCESSES						
chemical	0.0	1.5	0.1	0.1	0.0	0.0
food and agriculture	0.0	0.0	0.0	9.3	0.0	0.0
mineral processes	0.0	0.8	2.1	1.5	2.7	0.0
metal processes	0.0	0.0	0.0	0.0	0.0	0.0
wood and paper	0.0	0.0	0.5	0.0	0.0	0.0
glass and related products	0.0	0.0	0.0	10.0	0.0	0.0
electronics	0.0	0.0	0.0	0.0	0.0	0.0
other (industrial processes)	0.0	0.2	0.0	0.0	0.0	0.0
AREA-WIDE						
SOLVENT EVAPORATION						
consumer products	0.0	0.0	0.0	0.0	0.0	0.0
architectural coatings and related solvents	0.0	0.0	0.0	0.0	0.0	0.0
pesticides/fertilizers	0.0	0.0	0.0	0.0	0.0	0.0
asphalt paving	0.0	0.0	0.0	0.0	0.0	0.0
refrigerants	0.0	0.0	0.0	0.0	0.0	0.0
other (solvent evaporation)	0.0	0.0	0.0	0.0	0.0	0.0
MISCELLANEOUS PROCESSES						
residential fuel combustion	2.3	19.0	7.0	7.7	2.0	3.4
farming operations	0.0	0.0	0.0	0.0	0.0	0.0
construction and demolition	0.0	0.0	0.0	0.0	0.0	0.0
paved road dust	0.0	0.0	0.0	0.0	0.0	0.0
unpaved road dust	0.0	0.0	0.0	0.0	0.0	0.0
fugitive windblown dust	0.0	0.0	0.0	0.0	0.0	0.0
fires	0.0	0.1	0.0	0.1	0.0	0.0
waste burning and disposal	0.0	0.9	0.4	4.6	0.1	0.0
utility equipment	0.0	0.4	0.0	0.1	0.0	0.0
other (miscellaneous processes)	0.0	0.1	0.0	0.0	0.0	0.0

Table 2.3-2 (continued)
1996 Daily Average NOx Emissions by Air Basins in the CCOS Domain

SOURCE CATEGORIES	Mountain Counties	Bay Area	Sacramento Valley	San Joaquin Valley	North Central Coast	South Central Coast
MOBILE						
ON-ROAD MOTOR VEHICLES						
light duty passenger	11.4	134.8	53.7	71.2	13.0	29.8
light and medium duty trucks	0.0	0.0	0.0	0.0	0.0	0.0
light duty trucks	11.0	79.1	42.4	65.4	9.5	20.8
medium duty trucks	1.7	12.0	6.4	9.8	1.4	3.2
heavy duty gas trucks (all)	0.0	0.0	0.0	0.0	0.0	0.0
light heavy duty gas trucks	1.7	10.7	8.5	16.5	1.7	3.1
medium heavy duty gas trucks	0.5	3.6	2.8	5.4	0.6	1.0
heavy duty diesel trucks (all)	0.0	0.0	0.0	0.0	0.0	0.0
light heavy duty diesel trucks	0.6	5.0	4.1	5.7	0.8	1.3
medium heavy duty diesel trucks	1.3	11.3	9.1	12.8	1.9	3.0
heavy heavy duty diesel trucks	4.2	37.0	29.9	42.0	6.2	9.8
motorcycles	0.1	1.0	0.4	0.7	0.1	0.3
heavy duty diesel urban buses	0.0	5.2	0.7	0.8	0.4	0.3
other (on-road motor vehicles)	0.0	0.0	0.0	0.0	0.0	0.0
OTHER MOBILE SOURCES						
aircraft	0.0	22.0	2.1	3.1	0.3	0.5
trains	4.8	11.5	20.0	19.8	2.7	5.2
ships and commercial boats	0.0	11.4	0.2	0.3	0.1	4.2
recreational boats	0.5	0.3	0.9	0.9	0.1	0.4
off-road recreational vehicles	1.1	0.1	0.4	0.4	0.0	0.1
commercial/industrial mobile equipment	5.1	66.9	15.6	21.6	4.6	9.9
farm equipment	3.6	4.4	16.9	30.3	6.6	9.4
other (other mobile sources)	0.0	0.0	0.0	0.0	0.0	0.0
NATURAL (NON-ANTHROPOGENIC)						
geogenic sources	0.0	0.0	0.0	0.0	0.0	0.0
wildfires	0.6	0.0	0.8	0.9	0.4	1.2
windblown dust	0.0	0.0	0.0	0.0	0.0	0.0
other (natural sources)	0.0	0.0	0.0	0.0	0.0	0.0
TOTALS						
Stationary	5.8	102.6	28.2	184.1	20.2	14.8
Area-Wide	2.3	20.5	7.4	12.5	2.1	3.4
On-Road Motor Vehicles	32.5	299.7	158.0	230.3	35.6	72.6
Other Mobile Sources	15.1	116.6	56.1	76.4	14.4	29.7
Natural	0.6	0.0	0.8	0.9	0.4	1.2
TOTAL	56.3	539.4	250.5	504.2	72.7	121.7

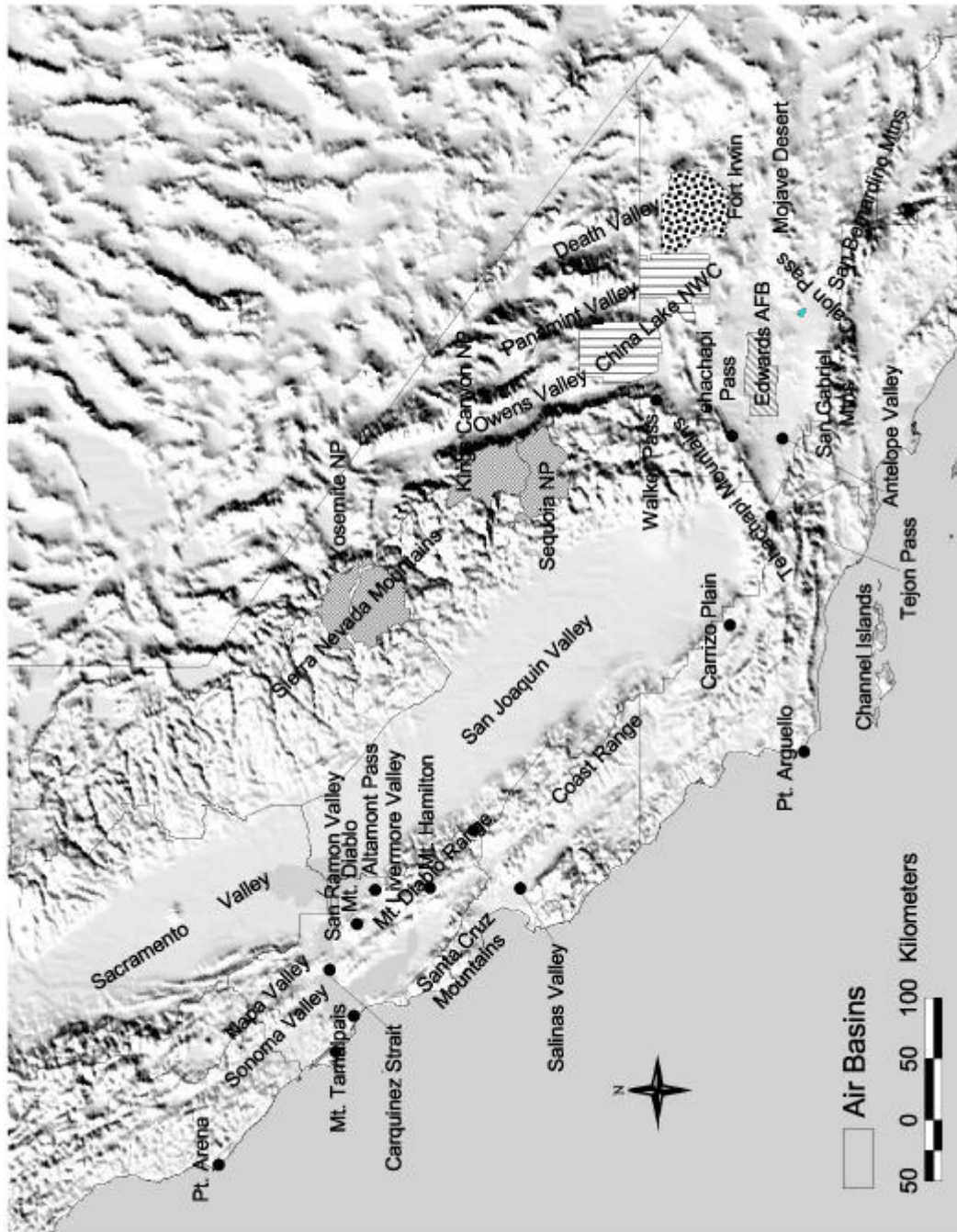


Figure 2.1-1. Overall study domain with major landmarks, mountains and passes.

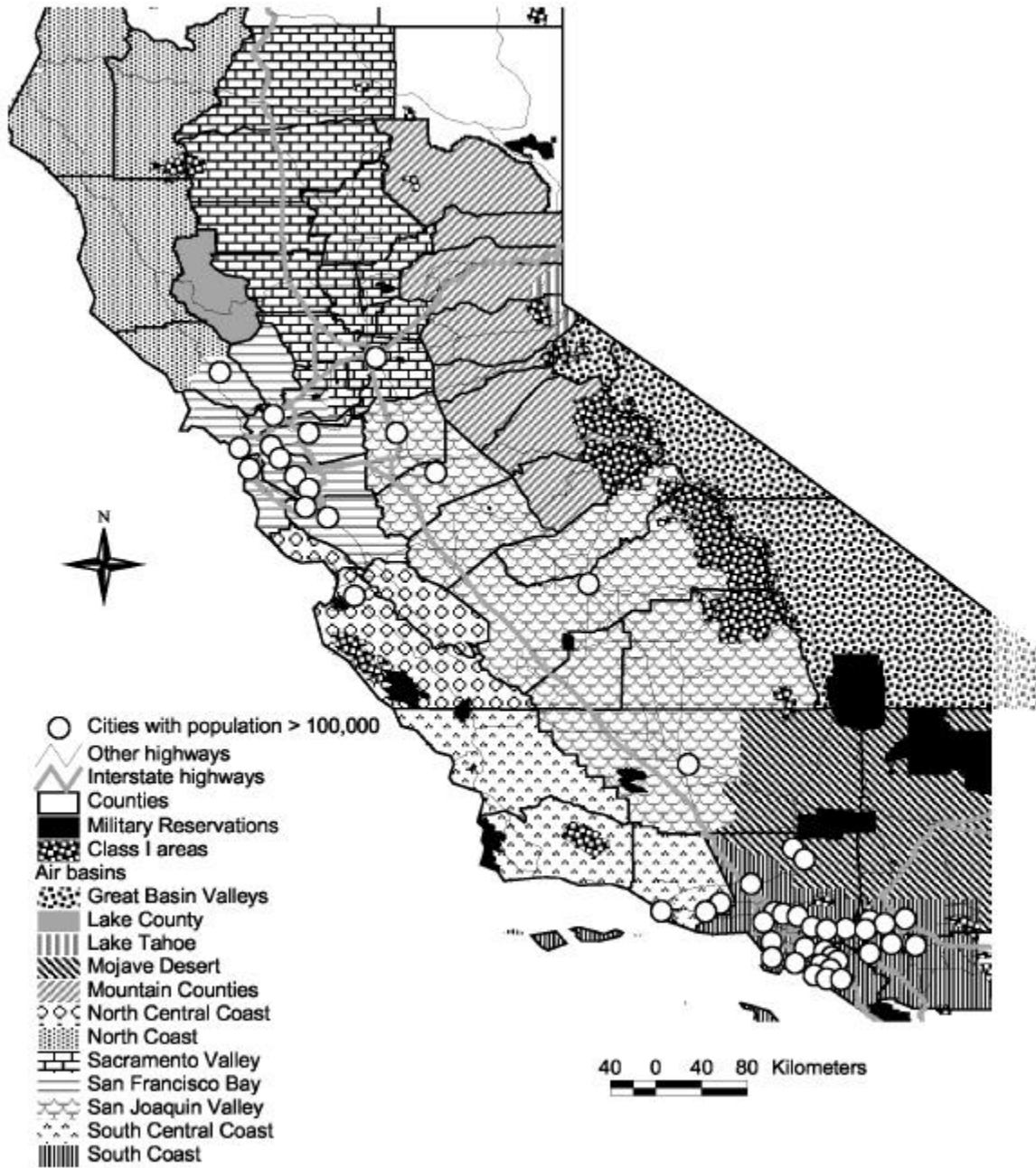


Figure 2.1-2. Major political boundaries and air basins within central California.

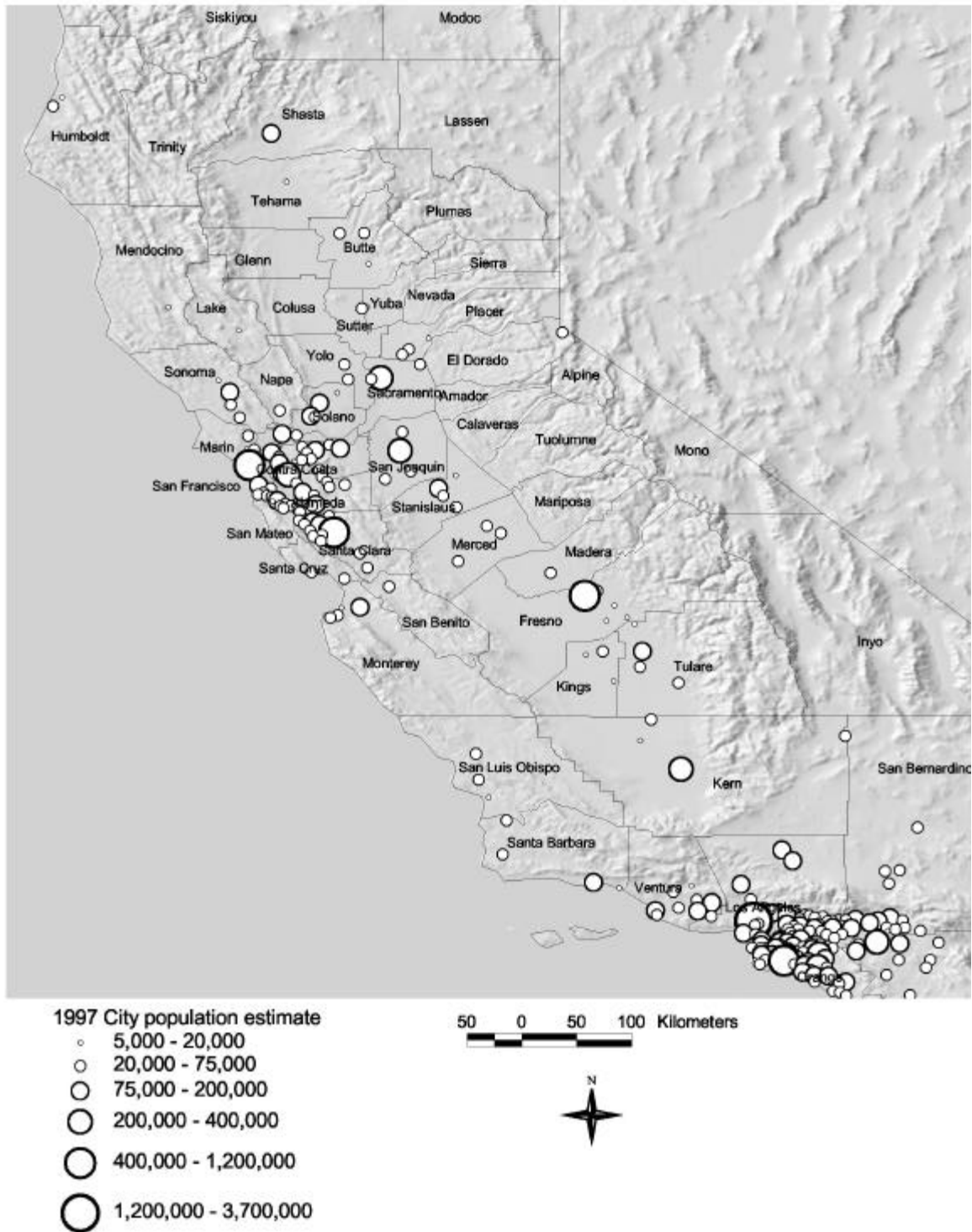


Figure 2.1-3. Major population centers within central California.

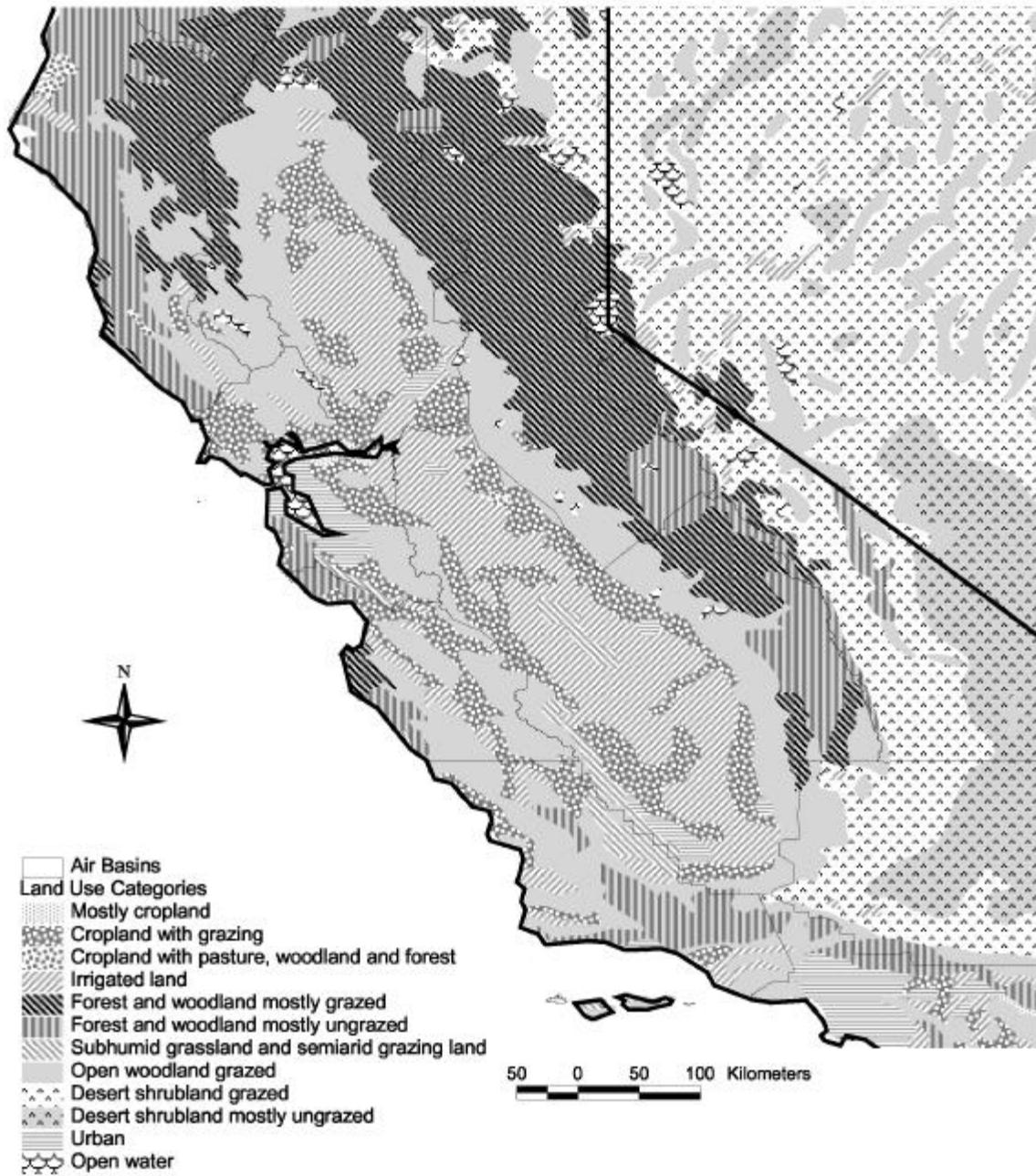


Figure 2.1-4. Land use within central California from the U.S. Geological Survey.

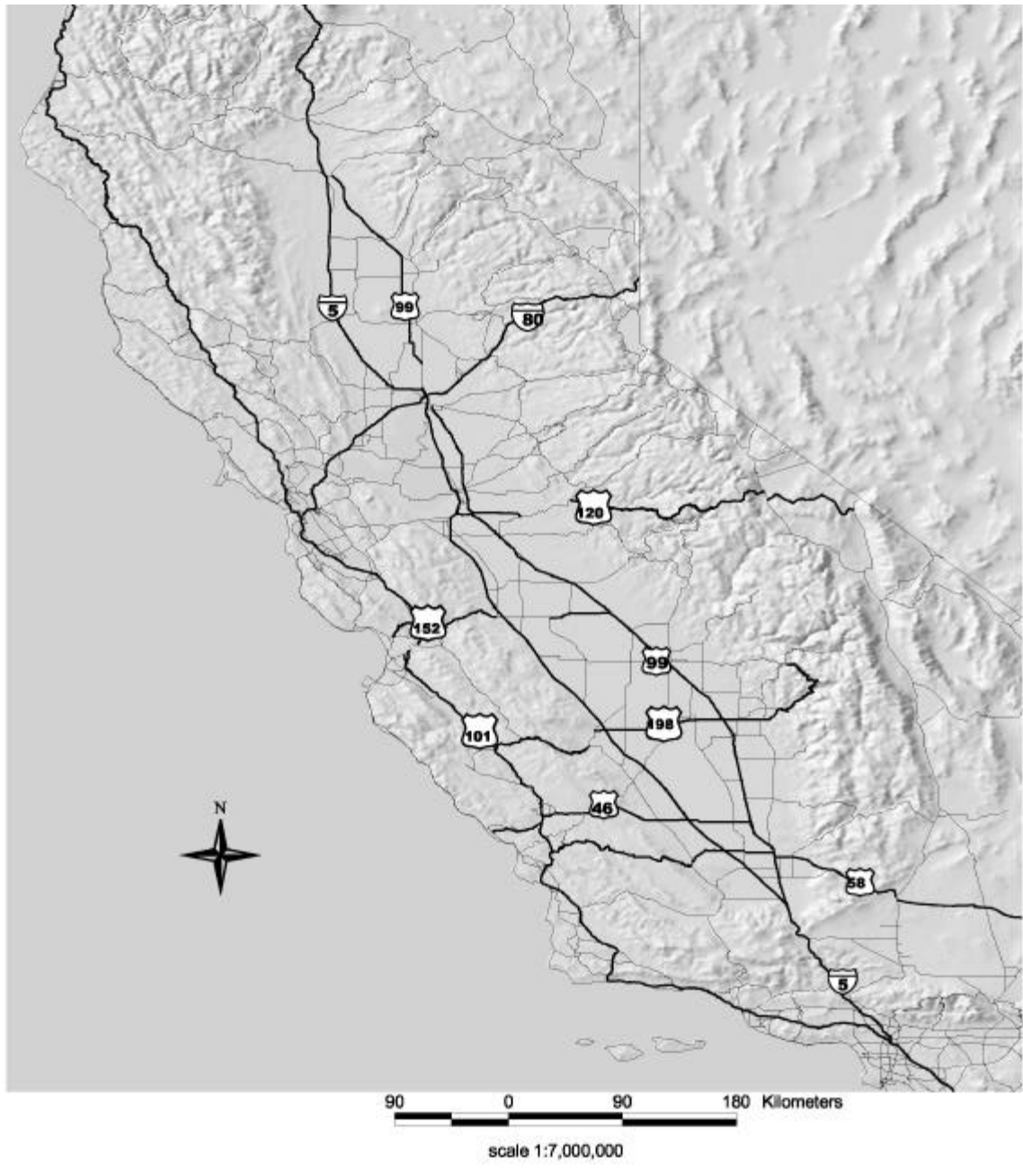
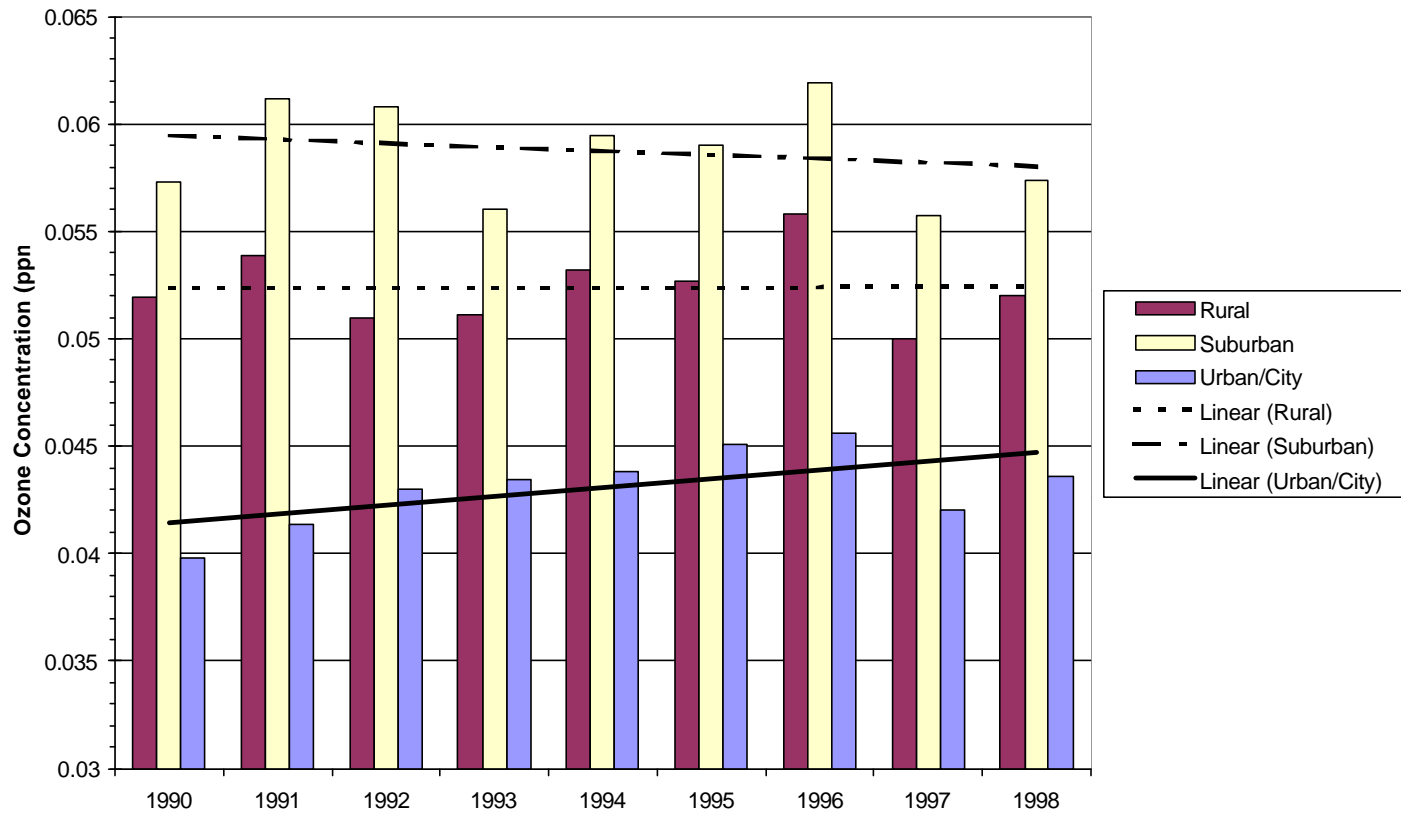


Figure 2.1-5. Major highway routes in central California.

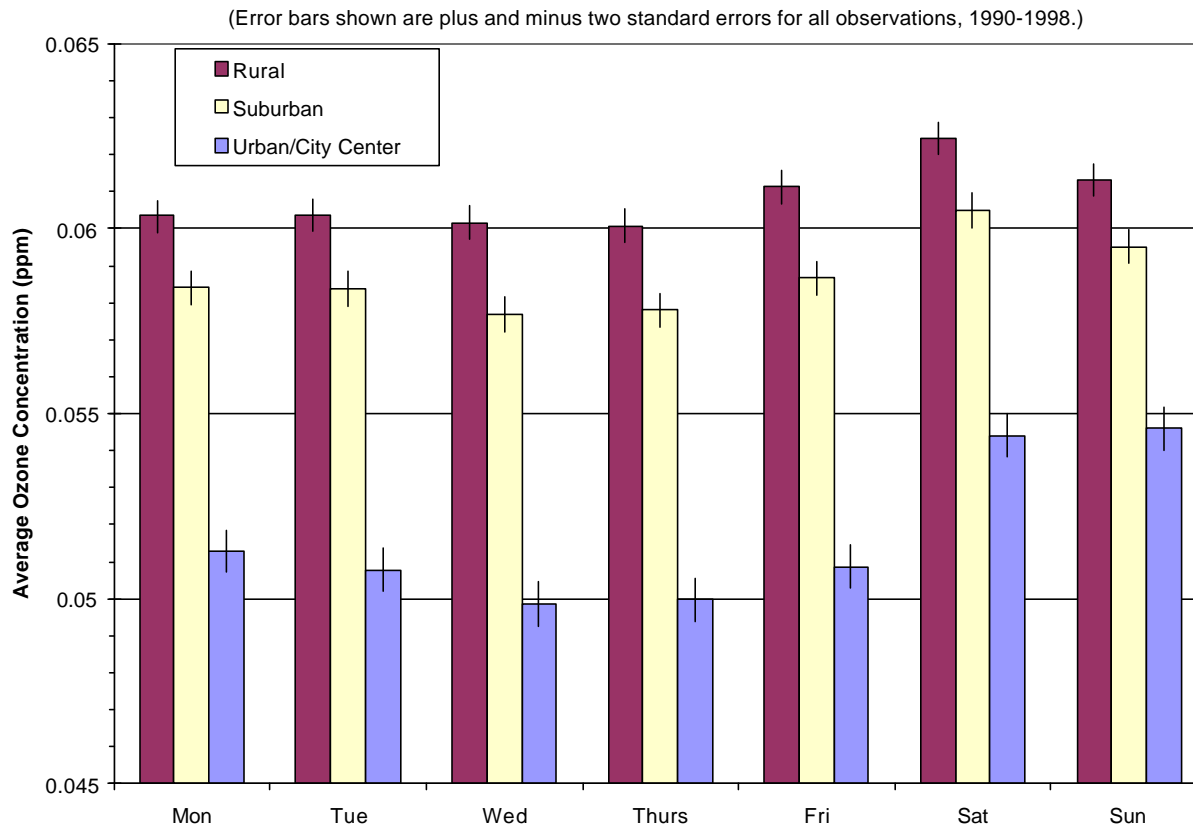
Ozone Trends in Central California by Location Type Average 8-Hr Daily Ozone Maxima



2-70

Figure 2.2-1. Average 8-hour daily maximum ozone trends in central California by location type.

Weekend/Weekday Effect in Central California, 1990-1998 Average Daily 1-Hour Ozone Maxima by Location Type



2-71

Figure 2.2-1. Weekend/weekday effect on average 1-hour daily maximum ozone in central California by location type.

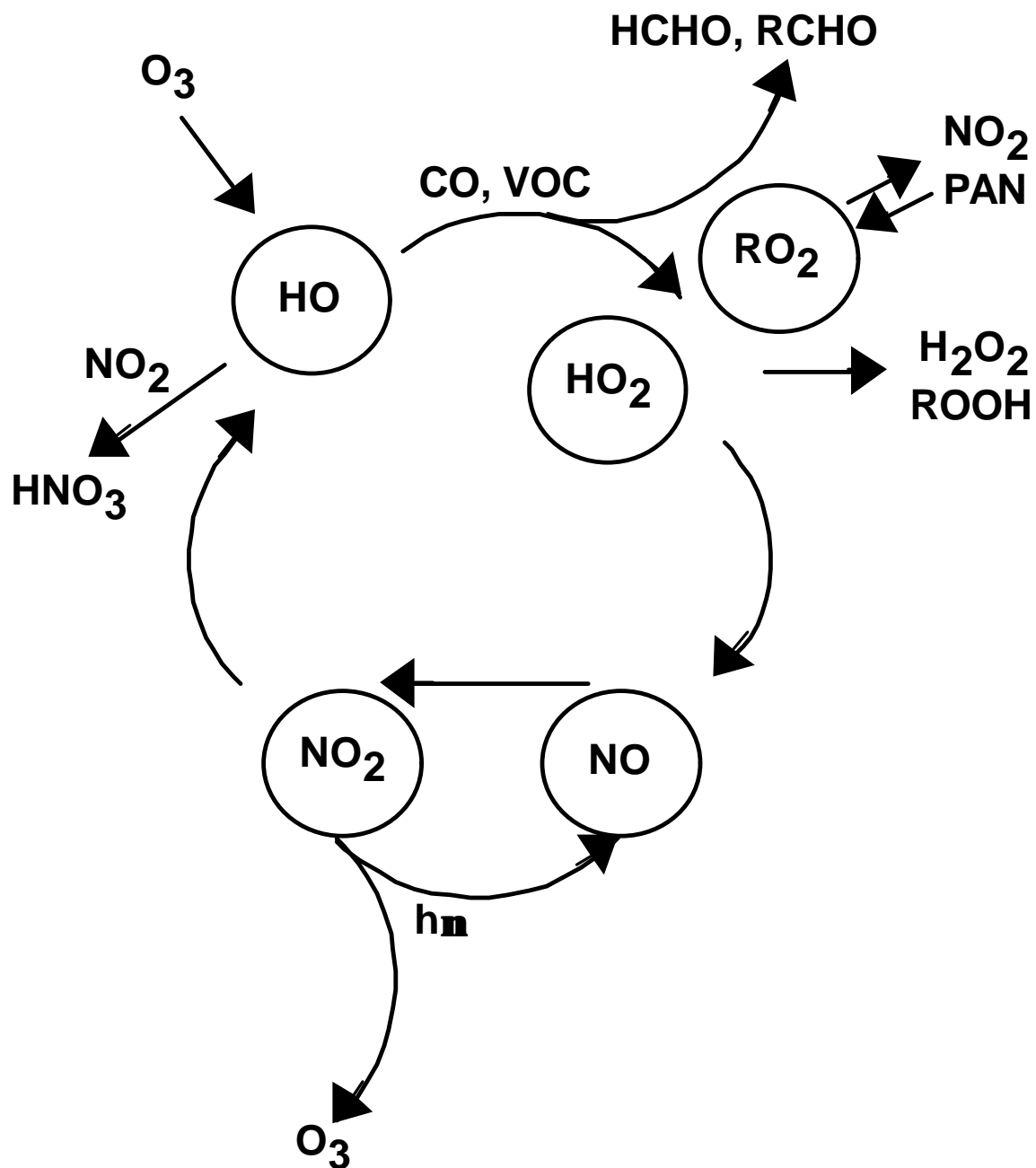


Figure 2.5-1. Overview of ozone production in the troposphere.

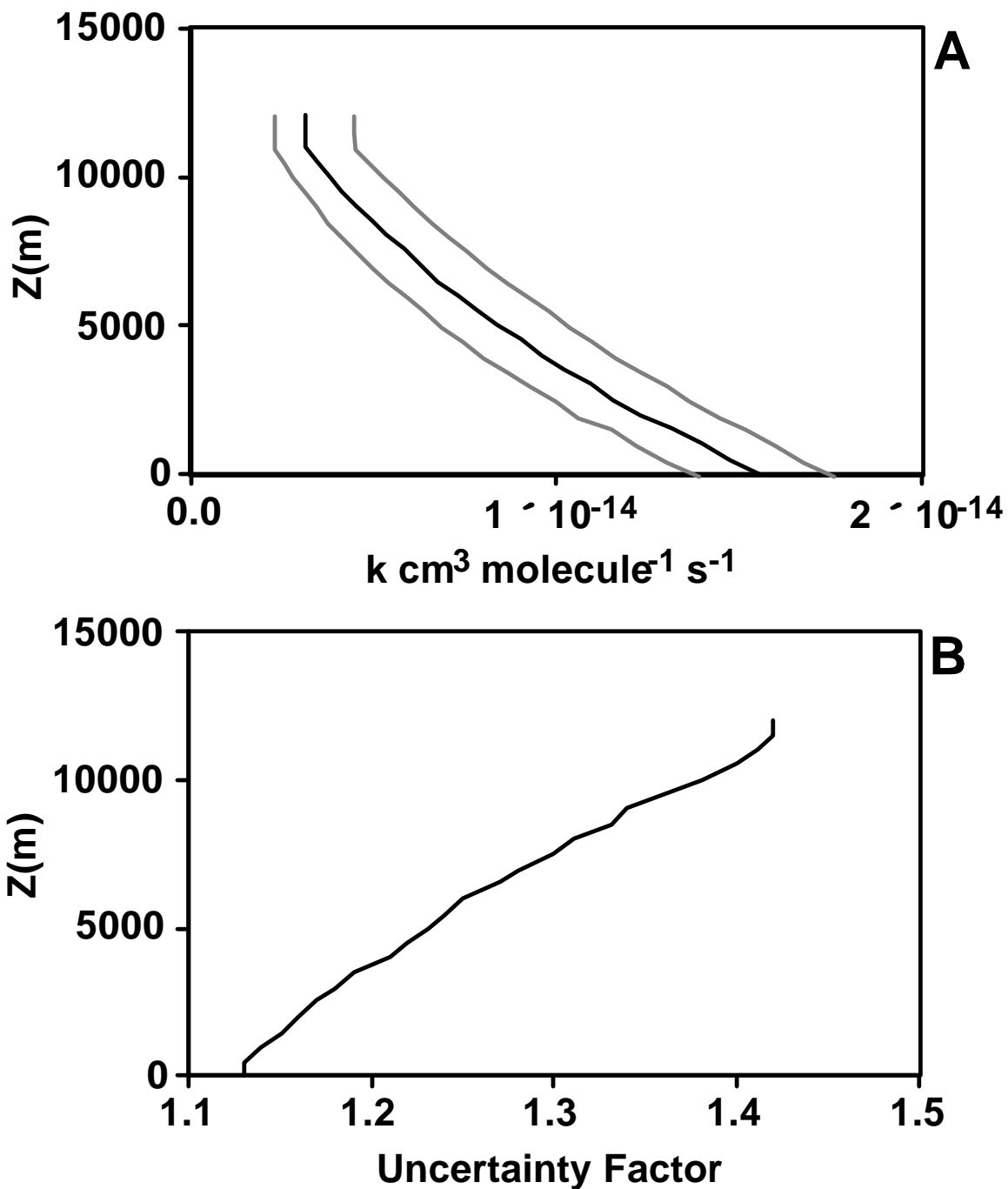


Figure 2.5-2. (A) Rate constant for the $\text{O}_3 + \text{NO}$ reaction with upper and lower bounds. (B) The uncertainty factor, $f(T)$. Data are from DeMore et al. (1997).

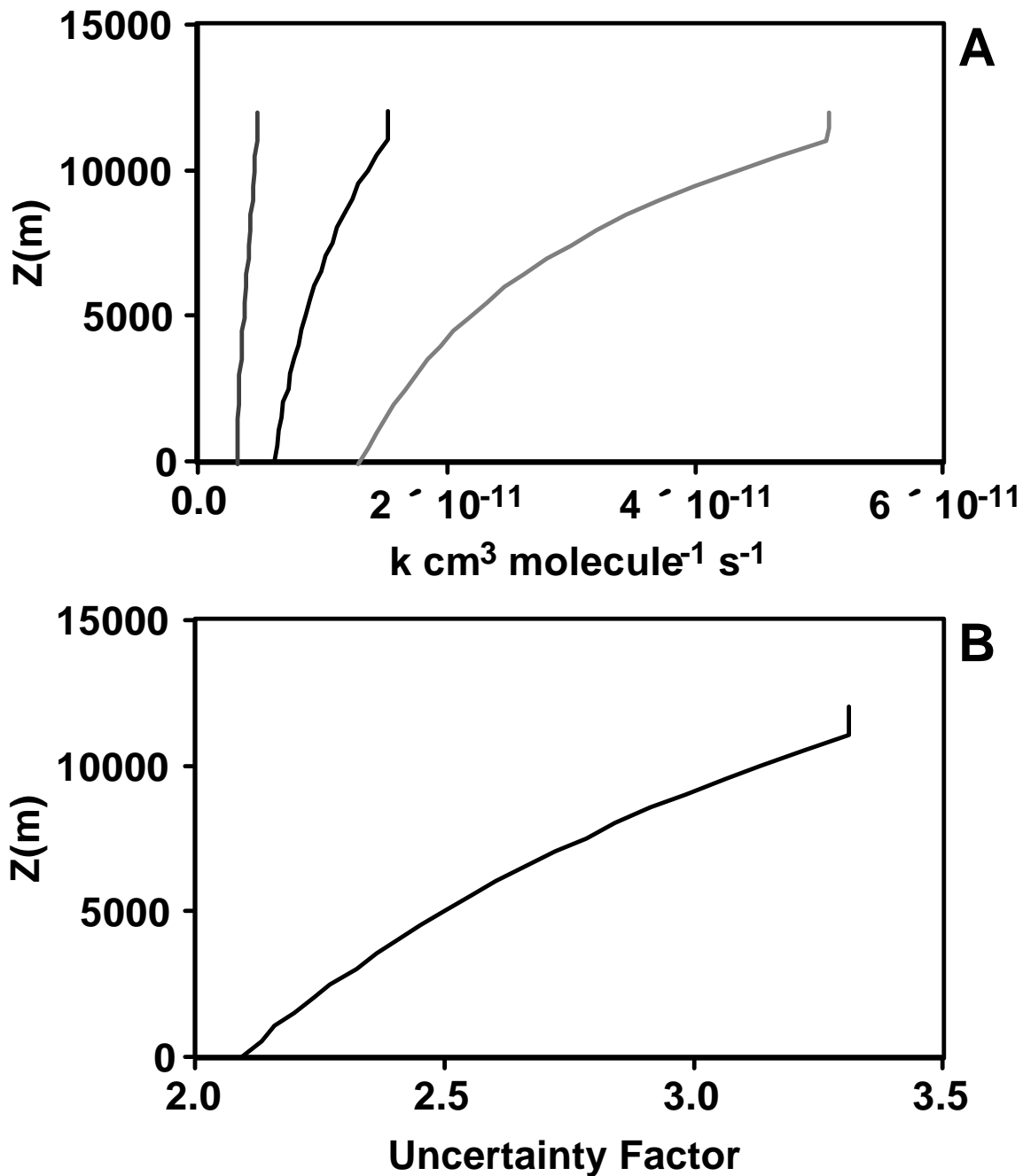


Figure 2.5-2. (A) Rate constant for the $\text{CH}_3\text{O}_2 + \text{HO}_2$ reaction with upper and lower bounds. (B) The uncertainty factor, $f(T)$. Data from DeMore et al. (1997).

2-75

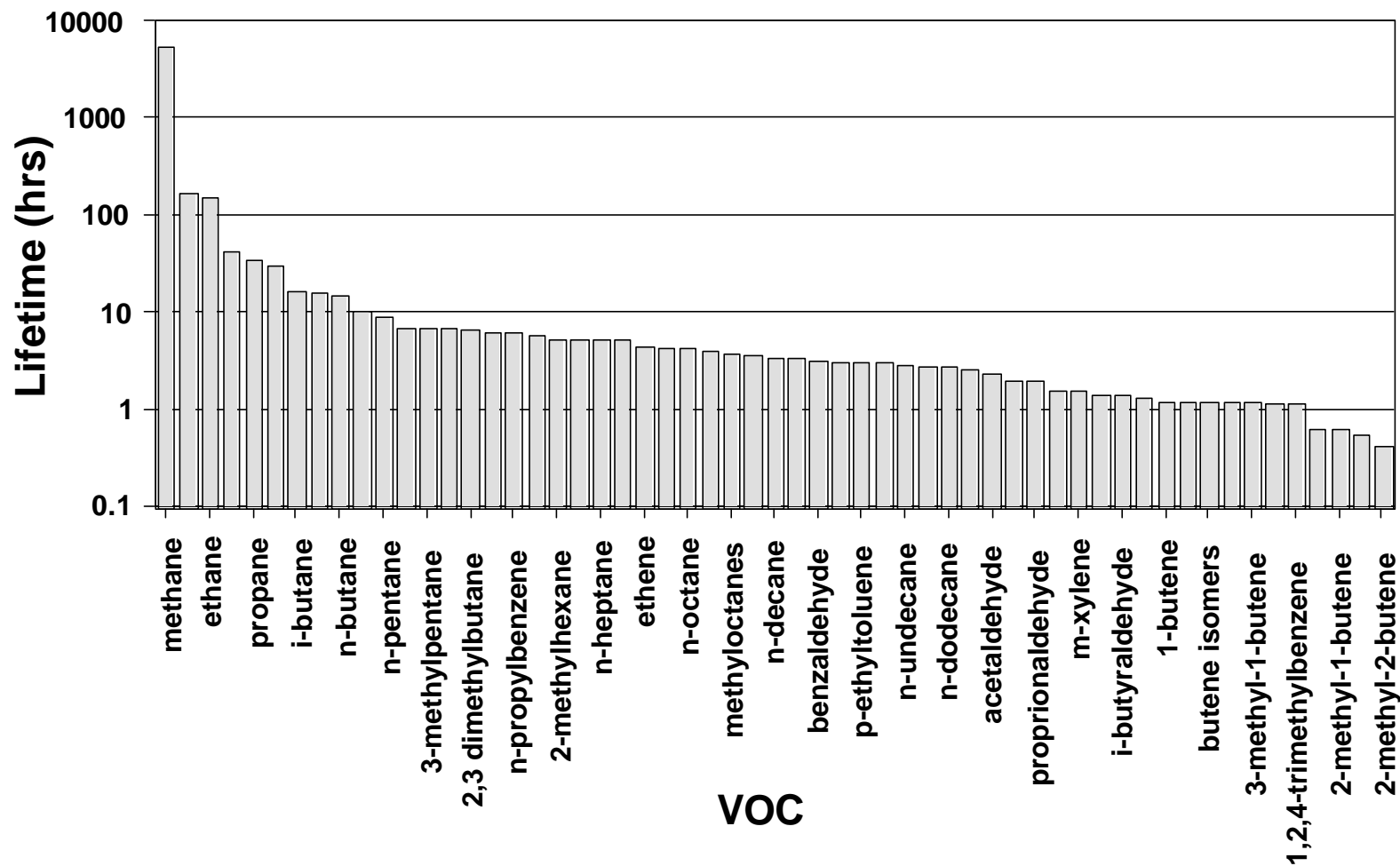


Figure 2.5-4. Atmospheric lifetimes of selected organic compounds with respect to a hydroxyl radical concentration of 7.5×10^6 molecules cm^{-3} .

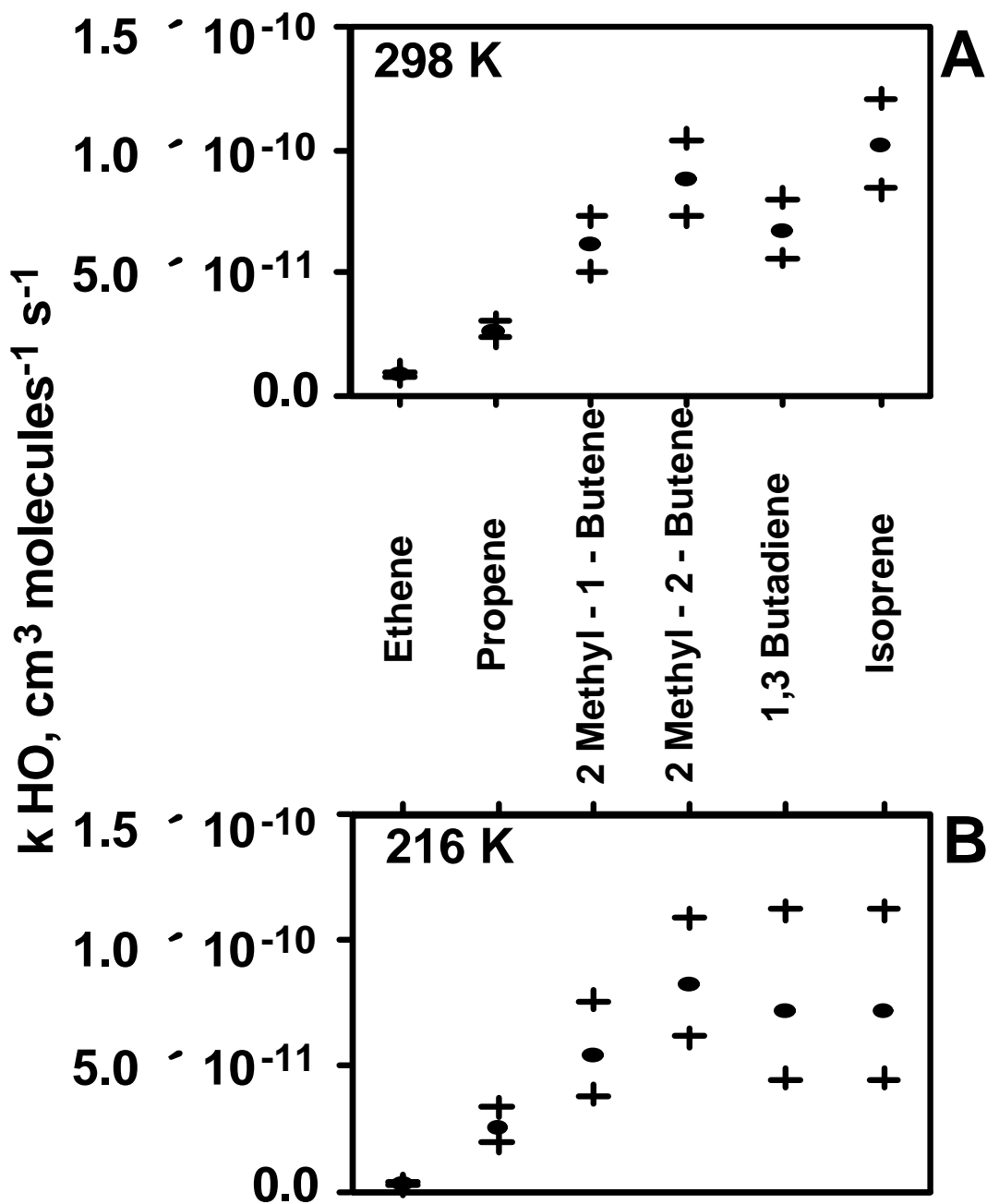


Figure 2.5-5. Uncertainties in rate parameters for HO radical reactions with alkenes. The closed circles represent the nominal value while the crosses represent the approximate 1σ; (A) 298 K; (B) 216 K.

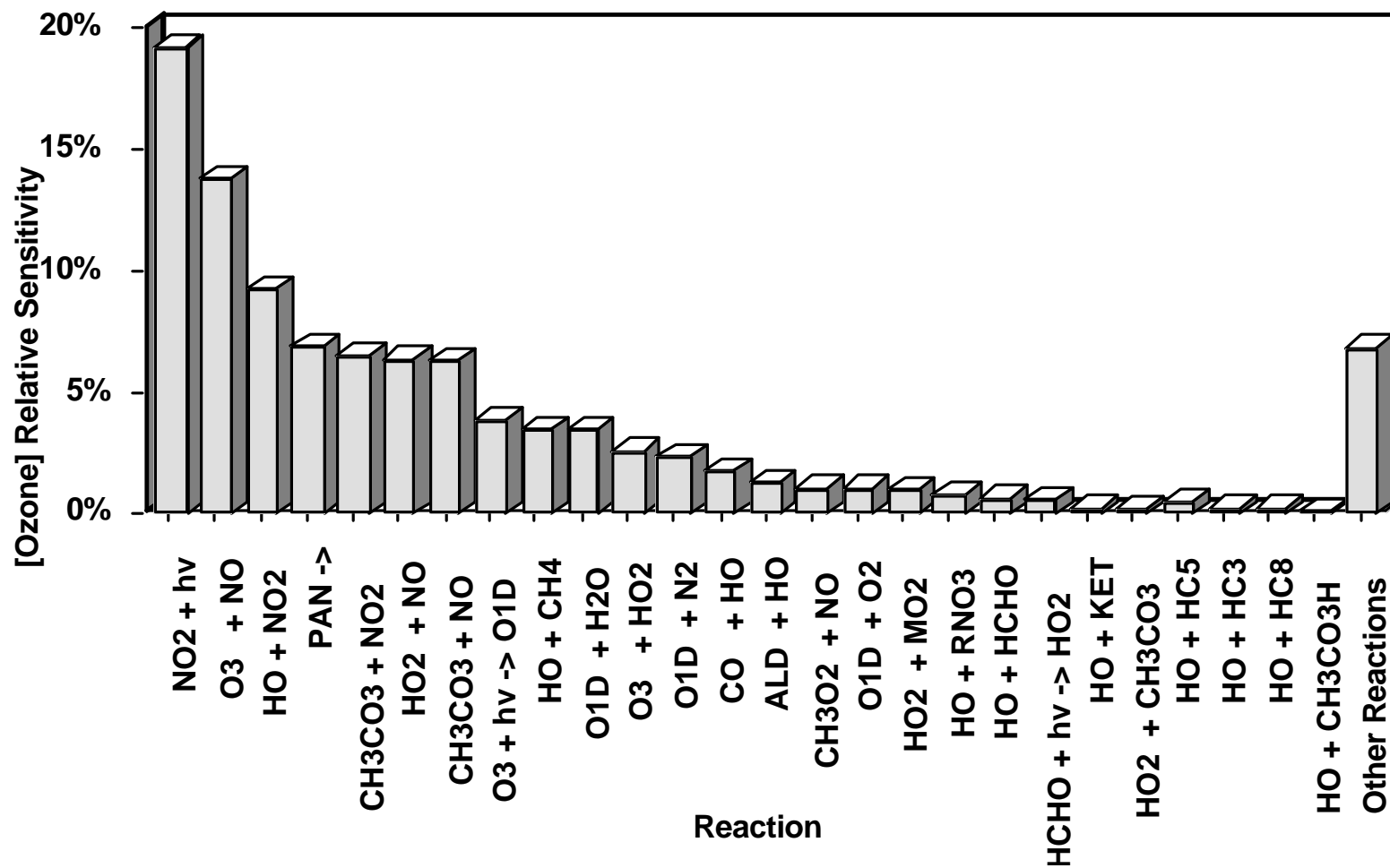


Figure 2.5-6. Relative sensitivity of ozone to reaction rate constants. Initial total reactive nitrogen concentration is 2 ppb and total initial organic compounds is 50 ppbC (Stockwell et al. 1995).

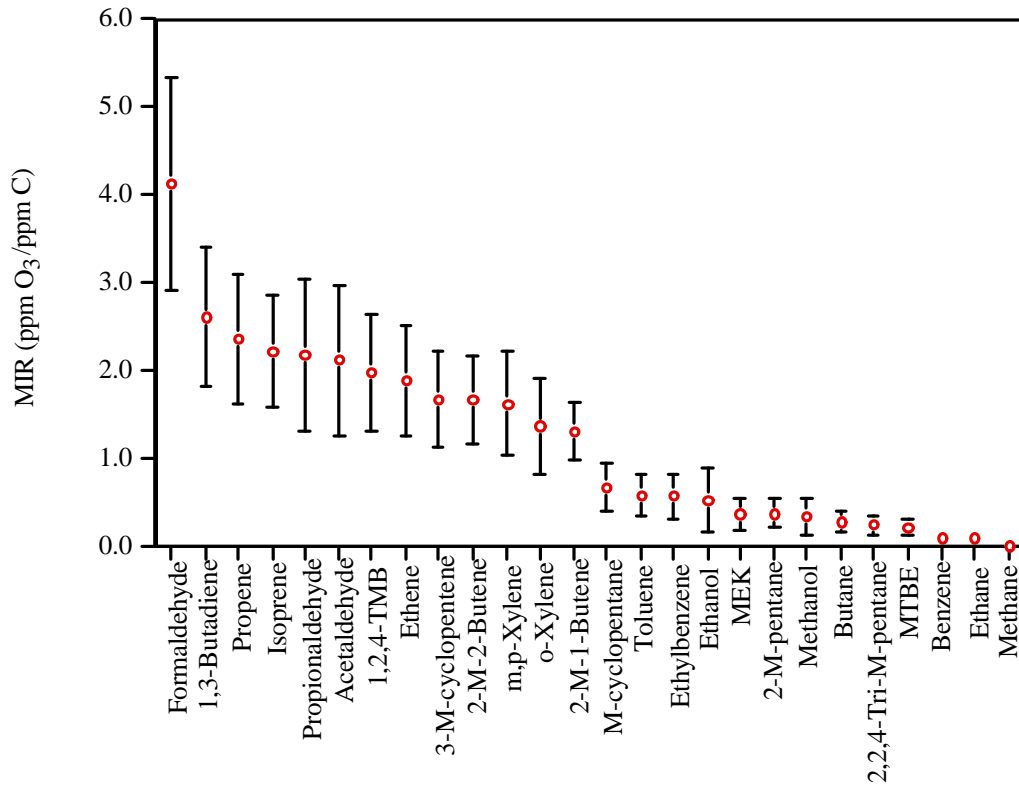


Figure 2.5-7. Mean values and 1σ uncertainties of maximum incremental reactivity values for selected hydrocarbons determined from Monte Carlo simulations (Yang et al., 1995).

**Table 2.6-1
Matrix of Meteorological Scenarios**

Type	Met Scenario Name	Description	Possible/Expected Mesoscale Features	May-Oct Frequency	Month Most Likely		
I	Western U.S. Hi	Ridge, off-shore gradient, weaker sea breeze		20.5%			
Ia	Pacific NW Hi (N Cal)			1.3%		Sep	
Ib	Great Basin Hi			5.3%		Aug	
Ic	Four Corners Hi			8.3%		Aug	
Id	Central or SoCal Hi			5.6%		Aug	
II	Eastern Pacific Hi	Broad ridge centered off-shore, sea breeze		8.9%			
IIa	North Hi (North of LA)			1.4%		Oct	
IIb	South Hi (LA or below)			3.4%		Jun	
IIc	w/ Cut-Off Lo to S			Can have a cut-off Lo, but check monsoonal		4.0%	Oct
III	Monsoonal Flow	Southeast flow brings gulf moisture		5.6%			
IIIa	Cut-Off Lo			5.4%		Jul	
IIIb	No Cut-Off Lo			0.2%		Jul (1case)	
IV	Zonal	West-to-East flow		15.4%			
IVa	Whole CA Coast			5.3%		May	
IVb	Hi in SE Pac or Mex			7.8%		June	
IVc	Lo in SE Pac or Mex			2.4%		May	
V	Pre-Frontal	Trough moving on-shore		18.5%			
Va	Whole CA Coast			7.1%		Jun	
Vb	North CA Coast			9.6%		Aug	
Vc	Cut-off Lo (SoCal coast)			1.8%		May	
VI	Trough Passage	Trough moves thru CA, NW-erlies follow		25.7%			
VIa	Whole CA Coast			16.5%		May	
VIb	North CA Coast			Hits SV and/or N SJV; not S SJV		2.7%	June
VIc	NW-erlies after trough			5.6%		Oct	
VId	Cut-off Lo			0.9%		Sep	
VII	Continental High	N wind, no marine air, more typical in winter		0.5%	Sep		
VIII	El Nino Cut-Off Lo	Persistent Lo off coast of SoCal or Mex		4.9%	Aug		

